Northumbria Research Link

Northumbria University NEWCASTLE

UniversityLibrary

Vibration and buckling behaviours of thin-walled composite and functionally graded sandwich I-beams

Ngoc-Duong Nguyen[a], Trung-Kien Nguyen[a,*], Thuc P. Vo[b], Thien-Nhan Nguyen[c], Seunghye Lee [d]

[a] Faculty of Civil Engineering, Ho Chi Minh City University of Technology and Education, 1 Vo Van Ngan Street, Thu Duc District, Ho Chi Minh City, Viet Nam.

[b] Faculty of Engineering and Environment, Northumbria University, Newcastle upon Tyne, NE1 8ST, UK.

[c] Faculty of Engineering and Technology, Kien Giang University, 320A Route 61, Kien Giang, Viet Nam.

[d] Department of Architectural Engineering, Sejong University 209, Neungdong-ro, Gwangjin-gu, Seoul 05006, Republic of Korea.

Abstract

The paper proposes a Ritz-type solution for free vibration and buckling analysis thin-walled composite and functionally graded sandwich I-beams. The variation of material through the thickness of functionally graded beams follows the power-law distribution. The displacement field is based on the first-order shear deformation theory, which can reduce to non-shear deformable one. The governing equations of motion are derived from Lagrange's equations. Ritz method is used to obtain the natural frequencies and critical buckling loads of thin-walled beams for both non-shear deformable and shear deformable theory. Numerical results are compared to those from previous works and investigate the effects of fiber angle, material distribution, span-to-height's ratio, and shear deformation on the critical buckling loads and natural frequencies of thin-walled I-beams for various boundary conditions.

Keywords: Ritz method; Vibration; Buckling; Thin-walled composite I-beams; Thin-walled functionally graded sandwich I-beams.

---

* Corresponding author. Tel.: + 848 3897 2092.
E-mail address: kiennt@hcmute.edu.vn (Trung-Kien Nguyen)

1. Introduction

In recent years, composite and functionally graded materials are commonly used in many fields of mechanical, aeronautical and civil engineering. The most well-known advantages of these materials are high stiffness-to-weight and strength-to-weight ratios, low thermal expansion, enhanced fatigue life and good corrosive resistance. In addition to their extensive use in practice, the available literatures indicate that a large number of studies have been conducted to analyse behaviours of these materials [1-3] in which thin-walled composite and functionally graded (FG) sandwich structures have been considered ([4-11]). One of the first thin-walled beam theories have been presented by Vlasov [12] and Gjelsvik [13]. Bauld and Lih-Shyng [14] then extended Vlasov's thin-walled beam theory of isotropic material to the composite one. Pandey et al. [15] used Galerkin's method to solve the equilibrium differential equation for analysing of the flexural-torsional buckling of thin-walled composite I-beams. Buckling and free vibration of these beams were presented by Lee and Kim [16, 17] based on the finite element method (FEM) and classical beam theory. The FEM was used by Rajasekaran and Nalinaa [18] to investigate static, buckling and vibration behaviours of thin-walled composite beams with generic section. Maddur and Chaturvedi [19, 20] presented a Vlasov-type modified first-order shear deformation theory (FSDT) and analysed the dynamic responses of thin-walled composite open sections beams. Qin and Librescu [21] used an extended Galerkin's method to investigate natural frequencies and static responses of anisotropic thin-walled beams which account for shear deformation effects. A beam element based on the first-order shear deformable beam theory was developed by Lee [22] for the bending analysis of laminated composite I-beams under uniformly distributed loads. Machado and Cortinez [23] presented a stability analysis of thin-

walled composite I-beams with open and closed sections considering shear deformation effects. Vo and Lee [24] extended previous resesearch [22] to study vibration and buckling of thin-walled open section composite beams. Dynamic stiffness matrix method also were used in the studies [25-28] to analyse vibration and buckling of the thin-walled composite beams. Silvestre and Camotim [29] used shear deformable generalised beam theory for buckling behaviours of lipped channel columns. Prokic et al. [30] proposed an analytical solution for free vibration of simply-supported thin-walled composite beams by using Vlasov's beam theory and classical lamination theory. Based on the Carrera Unified Formulation (CUF), Carrera et al. [31-35] analysed static, vibration and elastoplastic thin-walled composite structures. By using FEM, Sheikh et al. [36] conducted the study of free vibration of thin-walled composite beams having open and closed sections to investigate the shear effects. Li et al. [37] investigated hygrothermal effects on free vibration of simply-supported thin-walled composite beams by using Galerkin's method. Recently, the thin-walled FG beams have caught interests of many researchers. Nguyen et al. [38, 39] analysed vibration and lateral buckling of the thin-walled FG beams by FEM. Lanc et al. [40] analysed nonlinear buckling responses of thin-walled FG open section beams based on Euler-Bernoulli-Vlasov theory. Kim and Lee [41, 42] investigated the shear effects on free vibration and buckling behaviours of the thin-walled FG beam by three different types of finite beam elements, namely, linear, quadratic and cubic elements. The studies on the effects of shear deformation on buckling and vibration behaviours of thin-walled FG beams are still limited. On the other hand, Ritz method is simple and efficient to analyse the behaviours of composite beams with various boundary conditions [43-47], however, it has not been used for thin-walled composite and FG sandwich I-beams.

The main novelty of this work is to develop a Ritz solution for the vibration and buckling analyses of thin-walled composite and FG I-beams by using the first-order shear deformation beam theory. The governing equations of motion are derived by using Lagrange's equations. Results of the present element are compared with those in available literature to show its accuracy of the present solution. Parametric study is also performed to investigate the effects of shear deformation, span-to-height's ratio, fiber angle, material anisotropy and material distribution on natural frequencies and critical buckling loads of the thin-walled composite and FG sandwich I-beams.

2. Theoretical formulation

2.1. Kinematics

In this section, a kinematic field of the thin-walled composite and FG I-beams will be presented. The theoretical developments require three sets of coordinate systems as shown in Fig. 1 including the Cartesian coordinate system (x, y, z), local plate coordinate system (n, s, z) and contour coordinate s along the profile of the section. θ is an angle of orientation between (n, s, z) and (x, y, z) coordinate systems. The pole P, which has coordinate (x_P, y_P), is called the shear center [48].

The following assumptions are made:

    a. Strains are small and contour of section does not deform in its own plane.

    b. Shear strains $\gamma_{xz}^0, \gamma_{yz}^0$ and warping shear γ_{ϖ}^0 are uniform over the section.

    c. Local buckling and pre-buckling deformation is not considered.

    d. Poisson's coefficient is constant.

Relation of the mid-surface displacements $(\bar{u}, \bar{v}, \bar{w})$ at a point in the contour coordinate system and global beam displacements (U, V, W) is given by ([22]):

$$\bar{u}(s,z,t)=U(z,t)\sin\theta(s)-V(z,t)\cos\theta(s)-\phi(z,t)q(s) \tag{1a}$$

$$\bar{v}(s,z,t)=U(z,t)\cos\theta(s)+V(z,t)\sin\theta(s)+\phi(z,t)r(s) \tag{1b}$$

$$\bar{w}(s,z,t)=W(z,t)+\psi_y(z,t)x(s)+\psi_x(z,t)y(s)+\psi_\varpi(z,t)\varpi(s) \tag{1c}$$

where U, V and W are displacement of P in the $x-$, $y-$ and $z-$ direction, respectively; ϕ is the rotation angle about pole axis; ψ_x, ψ_y and ψ_ϖ denote rotations of the cross-section with respect to x, y and ϖ:

$$\psi_y=\gamma_{xz}^0-U' \tag{2a}$$

$$\psi_x=\gamma_{yz}^0-V' \tag{2b}$$

$$\psi_\varpi=\gamma_\varpi^0-\phi' \tag{2c}$$

where the prime superscript indicates differentiation with respect to z, and ϖ is warping function given by:

$$\varpi(s)=\int_{s_0}^{s}r(s)ds \tag{3}$$

The displacements (u,v,w) at any generic point on section are expressed by the mid-surface displacements $(\bar{u},\bar{v},\bar{w})$ as:

$$u(n,s,z,t)=\bar{u}(s,z,t) \tag{4a}$$

$$v(n,s,z,t)=\bar{v}(s,z,t)+n\bar{\psi}_s(s,z,t) \tag{4b}$$

$$w(n,s,z,t)=\bar{w}(s,z,t)+n\bar{\psi}_z(s,z,t) \tag{4c}$$

where $\bar{\psi}_s$ and $\bar{\psi}_z$ are determined by ([24]):

$$\bar{\psi}_z=\psi_y\sin\theta-\psi_x\cos\theta-\psi_\varpi q \tag{5a}$$

$$\bar{\psi}_s(s,z,t)=-\frac{\partial\bar{u}}{\partial s} \tag{5b}$$

6

The strain fields are defined as:

$$\varepsilon_s(n,s,z,t) = \bar{\varepsilon}_s(s,z,t) + n\bar{\kappa}_s(s,z,t) \tag{6a}$$

$$\varepsilon_z(n,s,z,t) = \bar{\varepsilon}_z(s,z,t) + n\bar{\kappa}_z(s,z,t) \tag{6b}$$

$$\gamma_{sz}(n,s,z,t) = \bar{\gamma}_{sz}(s,z,t) + n\bar{\kappa}_{sz}(s,z,t) \tag{6c}$$

$$\gamma_{nz}(n,s,z,t) = \bar{\gamma}_{nz}(s,z,t) + n\bar{\kappa}_{nz}(s,z,t) \tag{6d}$$

where

$$\bar{\varepsilon}_s = 0 \tag{7a}$$

$$\bar{\varepsilon}_z = \frac{\partial \bar{w}}{\partial z} = \varepsilon_z^0 + x\kappa_y + y\kappa_x + \varpi\kappa_\varpi \tag{7b}$$

$$\bar{\kappa}_s = 0 \tag{7c}$$

$$\bar{\kappa}_z = \frac{\partial \bar{\psi}_z}{\partial z} = \kappa_y \sin\theta - \kappa_x \cos\theta - \kappa_\varpi q \tag{7d}$$

$$\bar{\kappa}_{sz} = \kappa_{sz} \tag{7e}$$

$$\bar{\kappa}_{nz} = 0 \tag{7f}$$

$$\varepsilon_z^0 = W' \tag{7g}$$

$$\kappa_x = \psi'_x \tag{7h}$$

$$\kappa_y = \psi'_y \tag{7i}$$

$$\kappa_\varpi = \psi'_\varpi \tag{7j}$$

$$\kappa_{sz} = \phi' - \psi_\varpi \tag{7k}$$

$$\varepsilon_z = \varepsilon_z^0 + (x + n\sin\theta)\kappa_y + (y - n\cos\theta)\kappa_x + (\varpi - nq)\kappa_\varpi \tag{7l}$$

$$\gamma_{sz} = \gamma_{xz}^0 \cos\theta + \gamma_{yz}^0 \sin\theta + \gamma_\varpi^0 r + n\kappa_{sz} \tag{7m}$$

$$\gamma_{nz} = \gamma_{xz}^0 \sin\theta - \gamma_{yz}^0 \cos\theta - \gamma_\varpi^0 q \tag{7n}$$

2.2. Constitutive relations

2.2.1 Thin-walled composite beam

The composite beam is constituted by a finite number of orthotropic layers. The constitutive relation at the $k^{th} - $ layer in (n, s, z) coordinate systems can be expressed as:

$$\begin{Bmatrix} \sigma_z \\ \sigma_{sz} \\ \sigma_{nz} \end{Bmatrix}^{(k)} = \begin{pmatrix} \bar{Q}_{11}^* & \bar{Q}_{16}^* & 0 \\ \bar{Q}_{16}^* & \bar{Q}_{66}^* & 0 \\ 0 & 0 & \bar{Q}_{55}^* \end{pmatrix}^{(k)} \begin{Bmatrix} \varepsilon_z \\ \gamma_{sz} \\ \gamma_{nz} \end{Bmatrix} \tag{8}$$

where
$$\bar{Q}_{11}^* = \bar{Q}_{11} - \frac{\bar{Q}_{12}^2}{\bar{Q}_{22}} \tag{9a}$$

$$\bar{Q}_{16}^* = \bar{Q}_{16} - \frac{\bar{Q}_{12}\bar{Q}_{26}}{\bar{Q}_{22}} \tag{9b}$$

$$\bar{Q}_{66}^* = \bar{Q}_{66} - \frac{\bar{Q}_{26}^2}{\bar{Q}_{22}} \tag{9c}$$

$$\bar{Q}_{55}^* = \bar{Q}_{55} \tag{9d}$$

where $\bar{Q}_{ij}$ are the transformed reduced stiffnesses (see [49] for more details).

2.2.2. Thin-walled functionally graded (FG) sandwich beam

The constitutive relation of the FG sandwich I-beams can be written as follows:

$$\begin{Bmatrix} \sigma_z \\ \sigma_{sz} \\ \sigma_{nz} \end{Bmatrix} = \begin{pmatrix} \bar{Q}_{11}^* & 0 & 0 \\ 0 & \bar{Q}_{66}^* & 0 \\ 0 & 0 & \bar{Q}_{55}^* \end{pmatrix} \begin{Bmatrix} \varepsilon_z \\ \gamma_{sz} \\ \gamma_{nz} \end{Bmatrix} \tag{10}$$

where
$$\bar{Q}_{11}^* = E(n) \tag{11a}$$

$$\bar{Q}_{66}^* = \bar{Q}_{55}^* = \frac{E(n)}{2(1+\nu)} \tag{11b}$$

$E(n)$ is Young's modulus; ν is Poisson's coefficient. The effective mass density ρ and Young's modulus E of the thin-walled FG sandwich beam are approximated by:

$$\rho = \rho_c V_c + \rho_m \left(1 - V_c\right) \tag{12a}$$

$$E = E_c V_c + E_m \left(1 - V_c\right) \tag{12b}$$

where the subscripts c and m are used to indicate the ceramic and metal constituents, respectively; V_c is the volume fraction of ceramic material. Two type of material distributions are considered in this study:

Type A (for the flange, see Fig. 2b):

$$V_c = \left[\frac{n + 0.5h}{(1-\alpha)h}\right]^p, \quad -0.5h \leq n \leq (0.5-\alpha)h \tag{13a}$$

$$V_c = 1, \quad (0.5-\alpha)h \leq n \leq 0.5h \tag{13b}$$

where h $\left(h_1, h_2\right)$, p, α $\left(\alpha_1, \alpha_2\right)$ are the thickness of the flange, material parameter and thickness ratio of ceramic material of the flange, respectively.

Type B (for the web, see Fig. 2b):

$$V_c = \left[\frac{-|n| + 0.5h}{0.5(1-\beta)h}\right]^p, \quad -0.5h \leq n \leq -0.5\beta h \ \text{ or } \ 0.5\beta h \leq n \leq 0.5h \tag{14a}$$

$$V_c = 1, \quad -0.5\beta h \leq n \leq 0.5\beta h \tag{14b}$$

where $h = h_3$ is the thickness of the web; β is thickness ratio of the ceramic material of the web.

2.3. Variational formulation

The strain energy Π_E of the thin-walled beams is defined by:

$$\Pi_E = \frac{1}{2}\int_\Omega \left(\sigma_z \varepsilon_z + \sigma_{sz}\gamma_{sz} + k^s \sigma_{nz}\gamma_{nz}\right)d\Omega \tag{15a}$$

where k^s and Ω are shear correction factor and volume of beam, respectively. It is well-known that the models based on the first-order shear deformation theory require a

9

correct value of the shear correction factors. Several authors made contributions in order to improve the models used for the FSDT. Nguyen et al. [50] proposed shear correction factors for analysis of functionally graded beams and plates. Hutchinson [51], Gruttmann and Wagner [52], and Barbero et al. [53] presented formulas in order to compute the shear factors of different cross-sections of a Timoshenko's beam. In this paper, the shear factor is assumed to be a unity, which was suggested by some previous authors ([21, 22, 24]). Substituting Eqs. (7l), (7m), (7n), (8) and (10) into Eq. (15a) leads to:

$$
\begin{aligned}
\Pi_E = \frac{1}{2}\int_0^L \Big[& E_{11}W'^2 + 2E_{16}W'U' + 2E_{17}W'V' + 2(E_{15}+E_{18})W'\phi' \\
& +2E_{12}W'\psi_y' + 2E_{16}W'\psi_y + 2E_{13}W'\psi_x' + 2E_{17}W'\psi_x + 2E_{14}W'\psi_\varpi' \\
& +2(E_{18}-E_{15})W'\psi_\varpi + E_{66}U'^2 + 2E_{67}U'V' + 2(E_{56}+E_{68})U'\phi' + 2E_{26}U'\psi_y' \\
& +2E_{66}U'\psi_y + 2E_{36}U'\psi_x' + 2E_{67}U'\psi_x + 2E_{46}U'\psi_\varpi' + 2(E_{68}-E_{56})U'\psi_\varpi + E_{77}V'^2 \\
& +2(E_{57}+E_{78})V'\phi' + 2E_{27}V'\psi_y' + 2E_{67}V'\psi_y + 2E_{37}V'\psi_x' + 2E_{77}V'\psi_x + 2E_{47}V'\psi_\varpi' \\
& +2(E_{78}-E_{57})V'\psi_\varpi + (E_{55}+2E_{58}+E_{88})\phi'^2 + 2(E_{25}+E_{28})\phi'\psi_y' + 2(E_{56}+E_{68})\phi'\psi_y \\
& +2(E_{35}+E_{38})\phi'\psi_x' + 2(E_{57}+E_{78})\phi'\psi_x + 2(E_{45}+E_{48})\phi'\psi_\varpi' + 2(E_{88}-E_{55})\phi'\psi_\varpi \\
& +E_{22}\psi_y'^2 + 2E_{26}\psi_y'\psi_y + E_{66}\psi_y^2 + 2E_{23}\psi_y'\psi_x' + 2E_{27}\psi_y'\psi_x + 2E_{36}\psi_y\psi_x' + 2E_{67}\psi_y\psi_x \\
& +2E_{24}\psi_y'\psi_\varpi' + 2(E_{28}-E_{25})\psi_y'\psi_\varpi + 2E_{46}\psi_y\psi_\varpi' + 2(E_{68}-E_{56})\psi_y\psi_\varpi + E_{33}\psi_x'^2 \\
& +2E_{37}\psi_x'\psi_x + E_{77}\psi_x^2 + 2E_{34}\psi_x'\psi_\varpi' + 2(E_{38}-E_{35})\psi_x'\psi_\varpi + 2E_{47}\psi_x\psi_\varpi' \\
& +2(E_{78}-E_{57})\psi_x\psi_\varpi + E_{44}\psi_\varpi'^2 + 2(E_{48}-E_{45})\psi_\varpi'\psi_\varpi + (E_{88}-2E_{58}+E_{55})\psi_\varpi^2 \Big] dz
\end{aligned}
\tag{15b}
$$

where the stiffness coefficients E_{ij} are given in [24], L is length of beam.

The potential energy Π_W of thin-walled beam subjected to axial compressive load N_0 can be expressed as:

$$
\begin{aligned}
\Pi_W &= \frac{1}{2}\int_\Omega \frac{N_0}{A}\left(u'^2 + v'^2\right)d\Omega \\
&= \frac{1}{2}\int_0^L N_0\left(U'^2 + V'^2 + 2y_p U'\phi' - 2x_p V'\phi' + \frac{I_P}{A}\phi'^2\right)dz
\end{aligned}
\tag{16}
$$

where A is the cross-sectional area, I_P is polar moment of inertia of the cross-

section about the centroid defined by:

$$I_P = I_x + I_y \tag{17}$$

where I_x and I_y are second moment of inertia with respect to $x-$ and $y-$axis, defined by:

$$I_x = \int_A y^2 dA \tag{18a}$$

$$I_y = \int_A x^2 dA \tag{18b}$$

The kinetic energy Π_K of the thin-walled beam is given by:

$$
\begin{aligned}
\Pi_K &= \frac{1}{2} \int_\Omega \rho(n) \left(\dot{u}^2 + \dot{v}^2 + \dot{w}^2 \right) d\Omega \\
&= \frac{1}{2} \int_0^L \Big[m_0 \dot{W}^2 + 2m_s \dot{W}\dot{\psi}_y - 2m_c \dot{W}\dot{\psi}_x + 2\left(m_\varpi - m_q\right)\dot{W}\dot{\psi}_\varpi + m_0 \dot{U}^2 + 2\left(m_c + m_0 y_P\right)\dot{U}\dot{\phi} \\
&\quad + m_0 \dot{V}^2 + 2\left(m_s - m_0 x_p\right)\dot{V}\dot{\phi} + \left(m_p + m_2 + 2m_r\right)\dot{\phi}^2 + \left(m_{x2} + 2m_{xs} + m_{s2}\right)\dot{\psi}_y^2 \\
&\quad + 2\left(m_{xycs} - m_{cs}\right)\dot{\psi}_y\dot{\psi}_x + 2\left(m_{x\varpi} + m_{x\varpi qs} - m_{qs}\right)\dot{\psi}_y\dot{\psi}_\varpi + \left(m_{y2} - 2m_{yc} + m_{c2}\right)\dot{\psi}_x^2 \\
&\quad + 2\left(m_{y\varpi} - m_{y\varpi qc} + m_{qc}\right)\dot{\psi}_x\dot{\psi}_\varpi + \left(m_{\varpi 2} - 2m_{q\varpi} + m_{q2}\right)\dot{\psi}_\varpi^2 \Big] dz
\end{aligned}
\tag{19}
$$

where dot-superscript denotes the differentiation with respect to the time t, $\rho(n)$ is the mass density and the inertia coefficients are given in [24].

The total potential energy of thin-walled beam is expressed by:

$$\Pi = \Pi_E + \Pi_W - \Pi_K \tag{20}$$

2.4. Ritz solution

By using the Ritz method, the displacement field is approximated by:

$$W(z,t) = \sum_{j=1}^m \varphi_j'(z) W_j e^{i\omega t} \tag{21a}$$

$$U(z,t) = \sum_{j=1}^m \varphi_j(z) U_j e^{i\omega t} \tag{21b}$$

11

$$V(z,t) = \sum_{j=1}^{m} \varphi_j(z) V_j e^{i\omega t} \tag{21c}$$

$$\phi(z,t) = \sum_{j=1}^{m} \varphi_j(z) \phi_j e^{i\omega t} \tag{21d}$$

$$\psi_y(z,t) = \sum_{j=1}^{m} \varphi'_j(z) \psi_{yj} e^{i\omega t} \tag{21e}$$

$$\psi_x(z,t) = \sum_{j=1}^{m} \varphi'_j(z) \psi_{xj} e^{i\omega t} \tag{21f}$$

$$\psi_\varpi(z,t) = \sum_{j=1}^{m} \varphi'_j(z) \psi_{\varpi j} e^{i\omega t} \tag{21g}$$

where ω is the frequency, $i^2 = -1$ the imaginary unit; W_j, U_j, V_j, ϕ_j, ψ_{yj}, ψ_{xj} and $\psi_{\varpi j}$ are unknown and need to be determined; $\varphi_j(z)$ are shape functions, which satisfy the specified essential boundary conditions (BCs) [49]. It is clear that these shape functions in Table 1 satisfy various the BCs such as simply-supported (S-S), clamped-free (C-F) and clamped-clamped (C-C).

By substituting Eqs. (21) into Eq. (20) and using Lagrange's equations:

$$\frac{\partial \Pi}{\partial p_j} - \frac{d}{dt} \frac{\partial \Pi}{\partial \dot{p}_j} = 0 \tag{22}$$

with p_j representing the values of $\left(W_j, U_j, V_j, \phi_j, \psi_{yj}, \psi_{xj}, \psi_{\varpi j} \right)$, the vibration and buckling behaviours of the thin-walled beam can be obtained by solving the following equations:

$$
\left(
\begin{bmatrix}
\mathbf{K}^{11} & \mathbf{K}^{12} & \mathbf{K}^{13} & \mathbf{K}^{14} & \mathbf{K}^{15} & \mathbf{K}^{16} & \mathbf{K}^{17} \\
{}^{T}\mathbf{K}^{12} & \mathbf{K}^{22} & \mathbf{K}^{23} & \mathbf{K}^{24} & \mathbf{K}^{25} & \mathbf{K}^{26} & \mathbf{K}^{27} \\
{}^{T}\mathbf{K}^{13} & {}^{T}\mathbf{K}^{23} & \mathbf{K}^{33} & \mathbf{K}^{34} & \mathbf{K}^{35} & \mathbf{K}^{36} & \mathbf{K}^{37} \\
{}^{T}\mathbf{K}^{14} & {}^{T}\mathbf{K}^{24} & {}^{T}\mathbf{K}^{34} & \mathbf{K}^{44} & \mathbf{K}^{45} & \mathbf{K}^{46} & \mathbf{K}^{47} \\
{}^{T}\mathbf{K}^{15} & {}^{T}\mathbf{K}^{25} & {}^{T}\mathbf{K}^{35} & {}^{T}\mathbf{K}^{45} & \mathbf{K}^{55} & \mathbf{K}^{56} & \mathbf{K}^{57} \\
{}^{T}\mathbf{K}^{16} & {}^{T}\mathbf{K}^{26} & {}^{T}\mathbf{K}^{36} & {}^{T}\mathbf{K}^{46} & {}^{T}\mathbf{K}^{56} & \mathbf{K}^{66} & \mathbf{K}^{67} \\
{}^{T}\mathbf{K}^{17} & {}^{T}\mathbf{K}^{27} & {}^{T}\mathbf{K}^{37} & {}^{T}\mathbf{K}^{47} & {}^{T}\mathbf{K}^{57} & {}^{T}\mathbf{K}^{67} & \mathbf{K}^{77}
\end{bmatrix}
-\omega^2
\begin{bmatrix}
\mathbf{M}^{11} & 0 & 0 & 0 & \mathbf{M}^{15} & \mathbf{M}^{16} & \mathbf{M}^{17} \\
0 & \mathbf{M}^{22} & 0 & \mathbf{M}^{24} & 0 & 0 & 0 \\
0 & 0 & \mathbf{M}^{33} & \mathbf{M}^{34} & 0 & 0 & 0 \\
0 & {}^{T}\mathbf{M}^{24} & {}^{T}\mathbf{M}^{34} & \mathbf{M}^{44} & 0 & 0 & 0 \\
{}^{T}\mathbf{M}^{15} & 0 & 0 & 0 & \mathbf{M}^{55} & \mathbf{M}^{56} & \mathbf{M}^{57} \\
{}^{T}\mathbf{M}^{16} & 0 & 0 & 0 & {}^{T}\mathbf{M}^{56} & \mathbf{M}^{66} & \mathbf{M}^{67} \\
{}^{T}\mathbf{M}^{17} & 0 & 0 & 0 & {}^{T}\mathbf{M}^{57} & {}^{T}\mathbf{M}^{67} & \mathbf{M}^{77}
\end{bmatrix}
\right)
\begin{Bmatrix}
\mathbf{w} \\ \mathbf{u} \\ \mathbf{v} \\ \boldsymbol{\Phi} \\ \boldsymbol{\psi}_y \\ \boldsymbol{\psi}_x \\ \boldsymbol{\psi}_\varpi
\end{Bmatrix}
=
\begin{Bmatrix}
0 \\ 0 \\ 0 \\ 0 \\ 0 \\ 0 \\ 0
\end{Bmatrix}
\tag{23}
$$

where the stiffness matrix $\mathbf{K}$ and mass matrix $\mathbf{M}$ are expressed by:

$$
K_{ij}^{11} = E_{11}\int_0^L \varphi_i''\varphi_j'' dz , \quad
K_{ij}^{12} = E_{16}\int_0^L \varphi_i''\varphi_j' dz , \quad
K_{ij}^{13} = E_{17}\int_0^L \varphi_i''\varphi_j' dz , \quad
K_{ij}^{14} = \left(E_{15}+E_{18}\right)\int_0^L \varphi_i''\varphi_j' dz ,
$$

$$
K_{ij}^{15} = E_{12}\int_0^L \varphi_i''\varphi_j'' dz + E_{16}\int_0^L \varphi_i'\varphi_j' dz , \quad
K_{ij}^{16} = E_{13}\int_0^L \varphi_i''\varphi_j'' dz + E_{17}\int_0^L \varphi_i''\varphi_j' dz ,
$$

$$
K_{ij}^{17} = E_{14}\int_0^L \varphi_i''\varphi_j'' dz + \left(E_{18}-E_{15}\right)\int_0^L \varphi_i''\varphi_j' dz , \quad
K_{ij}^{22} = E_{66}\int_0^L \varphi_i'\varphi_j' dz + N_0\int_0^L \varphi_i'\varphi_j' dz , \quad
K_{ij}^{23} = E_{67}\int_0^L \varphi_i'\varphi_j' dz ,
$$

$$
K_{ij}^{24} = \left(E_{56}+E_{68}\right)\int_0^L \varphi_i'\varphi_j' dz + N_0 y_p\int_0^L \varphi_i'\varphi_j' dz , \quad
K_{ij}^{25} = E_{26}\int_0^L \varphi_i'\varphi_j'' dz + E_{66}\int_0^L \varphi_i'\varphi_j' dz ,
$$

$$
K_{ij}^{26} = E_{36}\int_0^L \varphi_i'\varphi_j'' dz + E_{67}\int_0^L \varphi_i'\varphi_j' dz , \quad
K_{ij}^{27} = E_{46}\int_0^L \varphi_i'\varphi_j'' dz + \left(E_{68}-E_{56}\right)\int_0^L \varphi_i'\varphi_j' dz ,
$$

$$
K_{ij}^{33} = E_{77}\int_0^L \varphi_i'\varphi_j' dz + N_0\int_0^L \varphi_i'\varphi_j' dz , \quad
K_{ij}^{34} = \left(E_{57}+E_{78}\right)\int_0^L \varphi_i'\varphi_j' dz - N_0 x_p\int_0^L \varphi_i'\varphi_j' dz ,
$$

$$
K_{ij}^{35} = E_{27}\int_0^L \varphi_i'\varphi_j'' dz + E_{67}\int_0^L \varphi_i'\varphi_j' dz , \quad
K_{ij}^{36} = E_{37}\int_0^L \varphi_i'\varphi_j'' dz + E_{77}\int_0^L \varphi_i'\varphi_j' dz ,
$$

$$
K_{ij}^{37} = E_{47}\int_0^L \varphi_i'\varphi_j'' dz + \left(E_{78}-E_{57}\right)\int_0^L \varphi_i'\varphi_j' dz , \quad
K_{ij}^{44} = \left(E_{55}+2E_{58}+E_{88}\right)\int_0^L \varphi_i'\varphi_j' dz + \frac{N_0 I_P}{A}\int_0^L \varphi_i'\varphi_j' dz ,
$$

$$K_{ij}^{45} = \left(E_{25} + E_{28}\right)\int_0^L \varphi_i^{'}\varphi_j^{''}dz + \left(E_{56} + E_{68}\right)\int_0^L \varphi_i^{'}\varphi_j^{'}dz \, ,$$

$$K_{ij}^{46} = \left(E_{35} + E_{38}\right)\int_0^L \varphi_i^{'}\varphi_j^{''}dz + \left(E_{57} + E_{78}\right)\int_0^L \varphi_i^{'}\varphi_j^{'}dz \, ,$$

$$K_{ij}^{47} = \left(E_{45} + E_{48}\right)\int_0^L \varphi_i^{'}\varphi_j^{''}dz + \left(E_{88} - E_{55}\right)\int_0^L \varphi_i^{'}\varphi_j^{'}dz \, ,$$

$$K_{ij}^{55} = E_{22}\int_0^L \varphi_i^{''}\varphi_j^{''}dz + E_{26}\int_0^L \left(\varphi_i^{''}\varphi_j^{'} + \varphi_i^{'}\varphi_j^{''}\right)dz + E_{66}\int_0^L \varphi_i^{'}\varphi_j^{'}dz \, ,$$

$$K_{ij}^{56} = E_{23}\int_0^L \varphi_i^{''}\varphi_j^{''}dz + E_{27}\int_0^L \varphi_i^{''}\varphi_j^{'}dz + E_{36}\int_0^L \varphi_i^{'}\varphi_j^{''}dz + E_{67}\int_0^L \varphi_i^{'}\varphi_j^{'}dz \, ,$$

$$K_{ij}^{57} = E_{24}\int_0^L \varphi_i^{''}\varphi_j^{''}dz + \left(E_{28} - E_{25}\right)\int_0^L \varphi_i^{''}\varphi_j^{'}dz + E_{46}\int_0^L \varphi_i^{'}\varphi_j^{''}dz + \left(E_{68} - E_{56}\right)\int_0^L \varphi_i^{'}\varphi_j^{'}dz \, ,$$

$$K_{ij}^{66} = E_{33}\int_0^L \varphi_i^{''}\varphi_j^{''}dz + E_{37}\int_0^L \left(\varphi_i^{''}\varphi_j^{'} + \varphi_i^{'}\varphi_j^{''}\right)dz + E_{77}\int_0^L \varphi_i^{'}\varphi_j^{'}dz \, ,$$

$$K_{ij}^{67} = E_{34}\int_0^L \varphi_i^{''}\varphi_j^{''}dz + \left(E_{38} - E_{35}\right)\int_0^L \varphi_i^{''}\varphi_j^{'}dz + E_{47}\int_0^L \varphi_i^{'}\varphi_j^{''}dz + \left(E_{78} - E_{57}\right)\int_0^L \varphi_i^{'}\varphi_j^{'}dz \, ,$$

$$K_{ij}^{77} = E_{44}\int_0^L \varphi_i^{''}\varphi_j^{''}dz + \left(E_{48} - E_{45}\right)\int_0^L \left(\varphi_i^{''}\varphi_j^{'} + \varphi_i^{'}\varphi_j^{''}\right)dz + \left(E_{88} - 2E_{58} + E_{55}\right)\int_0^L \varphi_i^{'}\varphi_j^{'}dz \, ,$$

$$M_{ij}^{11} = m_0\int_0^L \varphi_i^{'}\varphi_j^{'}dz \, , \quad M_{ij}^{15} = m_s\int_0^L \varphi_i^{'}\varphi_j^{'}dz \, , \quad M_{ij}^{16} = -m_c\int_0^L \varphi_i^{'}\varphi_j^{'}dz \, , \quad M_{ij}^{17} = \left(m_\varpi - m_q\right)\int_0^L \varphi_i^{'}\varphi_j^{'}dz \, ,$$

$$M_{ij}^{22} = m_0\int_0^L \varphi_i\varphi_j dz \, , \quad M_{ij}^{24} = \left(m_c + m_0 y_p\right)\int_0^L \varphi_i\varphi_j dz \, , \quad M_{ij}^{33} = m_0\int_0^L \varphi_i\varphi_j dz \, ,$$

$$M_{ij}^{34} = \left(m_s - m_0 x_p\right)\int_0^L \varphi_i\varphi_j dz \, , \quad M_{ij}^{44} = \left(m_p + m_2 + 2m_r\right)\int_0^L \varphi_i\varphi_j dz \, ,$$

$$M_{ij}^{55} = \left(m_{x2} + 2m_{xs} + m_{s2}\right)\int_0^L \varphi_i^{'}\varphi_j^{'}dz \, , \quad M_{ij}^{56} = \left(m_{xycs} - m_{cs}\right)\int_0^L \varphi_i^{'}\varphi_j^{'}dz \, ,$$

$$M_{ij}^{57} = \left(m_{x\varpi} + m_{x\varpi qs} - m_{qs}\right)\int_0^L \varphi_i^{'}\varphi_j^{'}dz \, , \quad M_{ij}^{66} = \left(m_{y2} - 2m_{yc} + m_{c2}\right)\int_0^L \varphi_i^{'}\varphi_j^{'}dz \, ,$$

$$M_{ij}^{67} = \left(m_{y\varpi} - m_{y\varpi qc} + m_{qc}\right)\int_0^L \varphi_i'\varphi_j' dz , \quad M_{ij}^{77} = \left(m_{\varpi 2} - 2m_{q\varpi} + m_{q2}\right)\int_0^L \varphi_i'\varphi_j' dz \tag{24}$$

If the shear effect is ignored, Eq. (2) degenerates to $\psi_y = -U'$, $\psi_x = -V'$, $\psi_\varpi = -\phi'$. By setting $\gamma_{xz}^0 = \gamma_{yz}^0 = \gamma_\varpi^0 = 0$ into the above equations, the number of unknown variables reduces to four (W, U, V, ϕ) as the Euler-Bernoulli-Vlasov beam model. Finally, the natural frequencies and critical buckling loads of the thin-walled beams without shear effects can be found:

$$\left(\begin{bmatrix} _{NS}\mathbf{K}^{11} & _{NS}\mathbf{K}^{12} & _{NS}\mathbf{K}^{13} & _{NS}\mathbf{K}^{14} \\ _{NS}^T\mathbf{K}^{12} & _{NS}\mathbf{K}^{22} & _{NS}\mathbf{K}^{23} & _{NS}\mathbf{K}^{24} \\ _{NS}^T\mathbf{K}^{13} & _{NS}^T\mathbf{K}^{23} & _{NS}\mathbf{K}^{33} & _{NS}\mathbf{K}^{34} \\ _{NS}^T\mathbf{K}^{14} & _{NS}^T\mathbf{K}^{24} & _{NS}^T\mathbf{K}^{34} & _{NS}\mathbf{K}^{44} \end{bmatrix} - \omega^2 \begin{bmatrix} _{NS}\mathbf{M}^{11} & \mathbf{0} & \mathbf{0} & \mathbf{0} \\ \mathbf{0} & _{NS}\mathbf{M}^{22} & \mathbf{0} & _{NS}\mathbf{M}^{24} \\ \mathbf{0} & \mathbf{0} & _{NS}\mathbf{M}^{33} & _{NS}\mathbf{M}^{34} \\ \mathbf{0} & _{NS}^T\mathbf{M}^{24} & _{NS}^T\mathbf{M}^{34} & _{NS}\mathbf{M}^{44} \end{bmatrix}\right) \begin{Bmatrix} \mathbf{w} \\ \mathbf{u} \\ \mathbf{v} \\ \mathbf{\Phi} \end{Bmatrix} = \begin{Bmatrix} \mathbf{0} \\ \mathbf{0} \\ \mathbf{0} \\ \mathbf{0} \end{Bmatrix} \tag{25}$$

where the stiffness matrix $\mathbf{K}$, mass matrix $\mathbf{M}$ are given by:

$$_{NS}K_{ij}^{11} = E_{11}\int_0^L \varphi_i''\varphi_j'' dz, \quad _{NS}K_{ij}^{12} = -E_{12}\int_0^L \varphi_i''\varphi_j'' dz, \quad _{NS}K_{ij}^{13} = -E_{13}\int_0^L \varphi_i''\varphi_j'' dz,$$

$$_{NS}K_{ij}^{14} = 2E_{15}\int_0^L \varphi_i''\varphi_j' dz - E_{14}\int_0^L \varphi_i''\varphi_j'' dz, \quad _{NS}K_{ij}^{22} = E_{22}\int_0^L \varphi_i''\varphi_j'' dz + N_0\int_0^L \varphi_i'\varphi_j' dz, \quad _{NS}K_{ij}^{23} = E_{23}\int_0^L \varphi_i''\varphi_j'' dz,$$

$$_{NS}K_{ij}^{24} = E_{24}\int_0^L \varphi_i''\varphi_j'' dz - 2E_{25}\int_0^L \varphi_i''\varphi_j' dz + N_0 y_p\int_0^L \varphi_i'\varphi_j' dz, \quad _{NS}K_{ij}^{33} = E_{33}\int_0^L \varphi_i''\varphi_j'' dz,$$

$$_{NS}K_{ij}^{34} = E_{34}\int_0^L \varphi_i''\varphi_j'' dz - 2E_{35}\int_0^L \varphi_i''\varphi_j' dz - N_0 x_p\int_0^L \varphi_i'\varphi_j' dz,$$

$$_{NS}K_{ij}^{44} = E_{44}\int_0^L \varphi_i''\varphi_j'' dz - 2E_{45}\left(\int_0^L \varphi_i''\varphi_j' dz + \int_0^L \varphi_i'\varphi_j'' dz\right) + 4E_{55}\int_0^L \varphi_i'\varphi_j' dz + \frac{N_0 I_p}{A}\int_0^L \varphi_i'\varphi_j' dz,$$

$$_{NS}M_{ij}^{11} = m_0\int_0^L \varphi_i'\varphi_j' dz, \quad _{NS}M_{ij}^{22} = m_0\int_0^L \varphi_i\varphi_j dz, \quad _{NS}M_{ij}^{24} = \left(m_c + m_0 y_p\right)\int_0^L \varphi_i\varphi_j dz,$$

$$_{NS}M_{ij}^{33} = m_0\int_0^L \varphi_i\varphi_j dz, \quad _{NS}M_{ij}^{34} = \left(m_s - m_0 x_p\right)\int_0^L \varphi_i\varphi_j dz, \quad _{NS}M_{ij}^{44} = \left(m_p + m_2 + 2m_\varpi\right)\int_0^L \varphi_i\varphi_j dz \tag{26}$$

3. Numerical results

Results for natural frequencies and critical buckling loads of thin-walled composite and FG sandwich I-beams with various configurations including boundary conditions, lay-ups and thickness ratio of the ceramic material are presented in this section. Convergence and comparison with the available literature are made to show the accuracy of the present solution. In addition, some new results, which may be used as reference data for future, are presented. The material properties and geometry of thin-walled I-beams are given in Table 2 and Fig. 2. The effect of the fiber angle, shear deformation, material parameter, span-to-height's ratio and thickness ratio of ceramic material on vibration and buckling behaviours of the thin-walled I-beams are investigated. The shear effect is defined by $(R_{NS} - R_s)/R_{NS} \times 100\%$ where R_S and R_{NS} denote the results with and without the shear effects, respectively.

Unless otherwise stated, the following non-dimensional terms are used:

$$\text{For composite I-beams:} \quad \bar{\omega} = \frac{\omega L^2}{b_3} \sqrt{\frac{\rho}{E_2}} \, , \quad \bar{N}_{cr} = \frac{N_{cr} L^2}{h E_2 b_3^3} \tag{27}$$

$$\text{For FG sandwich I-beams:} \quad \bar{\omega} = \frac{\omega L^2}{b_3} \sqrt{\frac{\rho_m}{E_m}} \, , \quad \bar{N}_{cr} = \frac{N_{cr} L^2}{h E_m b_3^3} \tag{28}$$

3.1. Convergence study

For purpose of testing convergence of present solution, the composite I-beams (MAT I, $b_1 = b_2 = b_3 = 5$ cm, $h_1 = h_2 = h_3 = 0.208$ cm and $L = 40b_3$) and FG sandwich I-beams (MAT III, $b_1 = b_2 = 15$ cm, $b_3 = 20$ cm, $h_1 = h_2 = h_3 = 0.5$ cm, $\alpha_1 = \alpha_2 = \beta = 0.1$, $p = 5$ and $L = 10b_3$) with the various BCs are considered. It is noted that both flanges and web of composite I-beams are assumed to be symmetrically laminated angle-ply

16

$[45/-45]_{4s}$ with respect to its mid-plane. The fundamental frequencies and critical buckling loads of thin-walled I-beams are presented in Table 3 with various series number m. As can be seen, a rapid convergence is obtained and $m=10$ is sufficient to guarantee the numerical convergence.

3.2. Composite I-beams

3.2.1. Example 1

The first example demonstrates accuracy and validity of present solutions. The symmetric angle-ply I-beams (MAT I) with the various BCs are considered. The flanges and web are 0.208 cm thickness, and made of symmetric laminates that consist of 16 layers ($[\eta/-\eta]_{4S}$). The first natural frequencies of S-S I-beams ($b_1 = b_2 = b_3 = 5$ cm and $L = 40b_3$), C-F I-beams ($b_1 = b_2 = 4$ cm, $b_5 = 5$ cm and $L = 20b_3$) and C-C I-beams ($b_1 = b_2 = b_3 = 5$ cm and $L = 40b_3$) are showed in Table 4 and Fig. 3. It can be seen that the present results are coincided with existing ones. The critical buckling loads of S-S I-beams ($b_1 = b_2 = b_3 = 5$ cm and $L = 80b_3$), C-F I-beams ($b_1 = b_2 = b_3 = 5$ cm and $L = 20b_3$) and C-C I-beams ($b_1 = b_2 = b_3 = 5$ cm, $L = 80b_3$) are displayed in Table 5 and Fig. 4, respectively. Good agreements between the present results and those of Vo and Lee [24], Kim et al. [27, 28] are found again. It is also stated that there are not much differences between shear and no shear results because these beams are slender.

3.2.2. Example 2

This example is to investigate the effects of shear deformation on the vibration and buckling behaviors of I-beams. The composite I-beams (MAT II, $b_1 = b_2 = 20$ cm, $b_3 = 30$ cm, $h_1 = h_2 = h_3 = 1$ cm and $L = 20b_3$) are considered. The top and bottom flanges are angle-ply lay-up $[\eta/-\eta]$ and the web is unidirectional one. The results of

I-beams with different BCs are displayed in Tables 6-9. From these tables, it can be seen that the present results comply with those of Vo and Lee [24], and both natural frequencies and critical buckling loads decrease as the fiber angle increases for all BCs. The shear effects of I-beams with $[15/-15]$ angle-ply in flanges for various BCs are conducted. Figs. 5 and 6 show the shear effects of fundamental frequencies and critical buckling load with respect to span-to-height's ratio, respectively. It can be seen that the shear effects are biggest for beams with C-C BCs, and are significant for beams with small span-to-height's ratio.

In order to clearly investigate the shear effects and fiber angle to the natural frequencies, the above composite I-beams with different geometry and material properties (MAT I, $b_1 = b_2 = b_3 = 30$ cm, $h_1 = h_2 = h_3 = 2$ cm and $L = 10b_3$) are considered. Fig. 7 displays the shear effects on first three frequencies of beams for C-C BC. It is clear to see that the shear effects are significant for high modes. It is also interesting to see that the shear effects on third mode (mode V) are smallest at fiber angle 55^0. This phenomenon can be explained in Fig. 8 which shows the ratio of flexural rigidity (E_{33}) to shear rigidity (E_{77}) with respect to η. It is observed that the ratio of E_{33}/E_{77} is the smallest at this angle (55^0). Figs. 9-11 also show first three mode shapes of C-C I-beams with $[45/-45]$ angle-ply in flanges with shear and without shear effect. It can be seen that the vibration modes 1, 2 and 3 are first flexural mode in $x-$direction (mode U), torsional mode (mode ϕ) and flexural mode in $y-$direction (mode V), respectively.

3.2.3. Example 3

The third example aims to investigate the effect of modulus ratio E_1/E_2 on natural frequencies and critical buckling loads of composite I- beams (MAT II, $b_1 = b_2 = 20$ cm,

18

$b_3 = 30$ cm, $h_1 = h_2 = h_3 = 1$ cm and $L = 20b_3$) with various BCs. The flanges are symmetric cross-ply $[0/90]_s$ lay-up and the web is unidirectional one. The variation of fundamental frequencies and critical buckling loads in case of including shear effects with respect to the ratio of E_1/E_2 is displayed in Figs. 12 and 13. It is observed that the results increase as E_1/E_2 increases for all BCs, and the beams with C-C BC have the biggest variation.

3.3. Functionally graded sandwich I-beams.

3.3.1. Example 4

This example is to assess the accuracy and efficiency of the present solution for thin-walled FG sandwich I-beams. Non-dimensional fundamental frequencies of S-S beams (MAT III, $b_1 = 20h$, $b_2 = 10h$, $b_3 = 40h$, $h_1 = h_2 = h_3 = h$, $\alpha_1 = 0.1$, $\alpha_2 = 0.9$ and $L = 40b_3$) with $p = 1$ and $p = 5$ are displayed in Fig 14. The critical buckling load of I-beams (MAT IV, $b_1 = b_2 = 10$ cm, $b_3 = 20$ cm, $h_1 = h_2 = h_3 = 0.5$ cm, $\alpha_1 = \alpha_2 = 0.7$, $\beta = 0.4$ and $L = 12.5b_3$) with different BCs is printed in Table 10. It can be found that the present solutions are in good agreements with previous results of Nguyen et al. [39], Lanc et al. [40] and Kim and Lee [41]. Results in Table 10 also indicated that the critical buckling loads decrease as material parameter p increases.

3.3.2. Example 5

In order to investigate the effects of thickness ratio of ceramic material on free vibration and buckling behaviours, the FG sandwich I-beams (MAT III, $b_1 = b_2 = 30h$, $b_3 = 40h$, $h_1 = h_2 = h_3 = h$ and $L = 10b_3$) are considered. Figs. 15 and 16 show the effect of ceramic thickness ratio in flanges on the non-dimensional fundamental frequencies and critical buckling loads of beams with $\beta = 0.3$ and $p = 10$ for the different BCs. It can

be seen that frequencies and critical buckling load significantly increase as ceramic thickness ratio increases. Figs. 17 and 18 show the non-dimensional fundamental frequencies and critical buckling loads of beams ($\alpha_1 = \alpha_1 = 0.1$ and $p = 10$) with respect to the ceramic thickness ratio in web for different BCs. It is observed that increasing of ceramic thickness ratio in web causes slightly decrease fundamental frequencies, and slightly increase critical loads.

3.3.3. Example 6

The FG sandwich I-beams (MAT III, $b_1 = b_2 = b_3 = 20h$, $h_1 = h_2 = h_3 = h$, $\alpha_1 = \alpha_2 = \beta = 0.1$) are considered to investigate the effects of shear deformation. Figs. 19 and 20 show shear effect on fundamental frequencies and critical buckling loads of beams with $p = 1$ and with respect to the span-to-height ratio. From these figures, it can be seen that the shear effects decrease as the span-to-height ratio increases as expected. Effects of the material parameter on the shear effects of the C-C I-beams with $L = 10b_3$ are indicated in Fig. 21. It can be seen that the shear effect is significant with high modes, and is not effected by the material parameter for first three vibration modes.

4. Conclusions

Ritz method is developed to analyse buckling and vibration of composite and FG sandwich I-beams in this paper. The theory is based on the first-order shear deformation theory. The governing equations of motion are derived from Lagrange's equations. Ritz shape functions are developed to solve problems. The natural frequencies, critical buckling loads of thin-walled composite and FG sandwich I-beams with various BCs are obtained and compared with those of the previous works. The results indicate that the present study is simply and significant for predicting buckling and vibration

20

behaviours of composite and FG sandwich I-beams.

References

1. Birman, V. and Kardomatea G.A., *Review of current trends in research and applications of sandwich structures.* Composites Part B: Engineering, 2018. **142**: p. 221-240.

2. Sayyad, A.S. and Ghugal Y.M., *Bending, buckling and free vibration of laminated composite and sandwich beams: A critical review of literature.* Composite Structures, 2017. **171**: p. 486-504.

3. Kreja, I., *A literature review on computational models for laminated composite and sandwich panels.* Open Engineering, 2011. **1**(1): p. 59-80.

4. Nguyen, T.-T. and Lee J., *Flexural-torsional vibration and buckling of thin-walled bi-directional functionally graded beams.* Composites Part B: Engineering, 2018. **154**: p. 351-362.

5. Nguyen, T.-T. and Lee J., *Interactive geometric interpretation and static analysis of thin-walled bi-directional functionally graded beams.* Composite Structures, 2018. **191**: p. 1-11.

6. Vukasović, M., Pavazza R., and Vlak F., *An analytic solution for bending of thin-walled laminated composite beams of symmetrical open sections with influence of shear.* The Journal of Strain Analysis for Engineering Design, 2017. **52**(3): p. 190-203.

7. Nguyen, T.-T., Kim N.-I., and Lee J., *Analysis of thin-walled open-section beams with functionally graded materials.* Composite Structures, 2016. **138**: p. 75-83.

8. Nguyen, H.X., Lee J., Vo T.P., and Lanc D., *Vibration and lateral buckling optimisation of thin-walled laminated composite channel-section beams.* Composite

Structures, 2016. **143**: p. 84-92.

9. Kim, N.-I. and Lee J., *Exact solutions for stability and free vibration of thin-walled Timoshenko laminated beams under variable forces.* Archive of Applied Mechanics, 2014. **84**(12).

10. Piovan, M.T., Ramirez J.M., and Sampaio R., *Dynamics of thin-walled composite beams: Analysis of parametric uncertainties.* Composite Structures, 2013. **105**: p. 14-28.

11. Kim, N.-I. and Lee J., *Improved torsional analysis of laminated box beams.* Meccanica, 2013. **48**(6): p. 1369-1386.

12. Vlasov, V., *Thin-walled elastic beams. Israel program for scientific translations, Jerusalem.* 1961, Oldbourne Press, London.

13. Gjelsvik, A., *The theory of thin walled bars*. 1981: Krieger Pub Co.

14. Bauld, N.R. and Lih-Shyng T., *A Vlasov theory for fiber-reinforced beams with thin-walled open cross sections.* International Journal of Solids and Structures, 1984. **20**(3): p. 277-297.

15. Pandey, M.D., Kabir M.Z., and Sherbourne A.N., *Flexural-torsional stability of thin-walled composite I-section beams.* Composites Engineering, 1995. **5**(3): p. 321-342.

16. Lee, J. and Kim S.-E., *Free vibration of thin-walled composite beams with I-shaped cross-sections.* Composite structures, 2002. **55**(2): p. 205-215.

17. Lee, J. and Kim S.-E., *Flexural–torsional buckling of thin-walled I-section composites.* Computers & Structures, 2001. **79**(10): p. 987-995.

18. Rajasekaran, S. and Nalinaa K., *Stability and vibration analysis of non-prismatic thin-walled composite spatial members of generic section.* International Journal of

Structural Stability and Dynamics, 2005. **5**(04): p. 489-520.

19. Maddur, S.S. and Chaturvedi S.K., *Laminated composite open profile sections: non-uniform torsion of I-sections.* Composite Structures, 2000. **50**(2): p. 159-169.

20. Maddur, S.S. and Chaturvedi S.K., *Laminated composite open profile sections: first order shear deformation theory.* Composite Structures, 1999. **45**(2): p. 105-114.

21. Qin, Z. and Librescu L., *On a shear-deformable theory of anisotropic thin-walled beams: further contribution and validations.* Composite Structures, 2002. **56**(4): p. 345-358.

22. Lee, J., *Flexural analysis of thin-walled composite beams using shear-deformable beam theory.* Composite Structures, 2005. **70**(2): p. 212-222.

23. Machado, S.P. and Cortínez V.H., *Non-linear model for stability of thin-walled composite beams with shear deformation.* Thin-Walled Structures, 2005. **43**(10): p. 1615-1645.

24. Vo, T.P. and Lee J., *Flexural–torsional coupled vibration and buckling of thin-walled open section composite beams using shear-deformable beam theory.* International Journal of Mechanical Sciences, 2009. **51**(9): p. 631-641.

25. Kim, N.-I. and Shin D.K., *Dynamic stiffness matrix for flexural-torsional, lateral buckling and free vibration analyses of mono-symmetric thin-walled composite beams.* International Journal of Structural Stability and Dynamics, 2009. **9**(03): p. 411-436.

26. Kim, N.-I., Shin D.K., and Park Y.-S., *Dynamic stiffness matrix of thin-walled composite I-beam with symmetric and arbitrary laminations.* Journal of Sound and Vibration, 2008. **318**(1): p. 364-388.

27. Kim, N.-I., Shin D.K., and Kim M.-Y., *Flexural–torsional buckling loads for*

spatially coupled stability analysis of thin-walled composite columns. Advances in Engineering Software, 2008. **39**(12): p. 949-961.

28. Kim, N.-I., Shin D.K., and Kim M.-Y., *Improved flexural–torsional stability analysis of thin-walled composite beam and exact stiffness matrix.* International journal of mechanical sciences, 2007. **49**(8): p. 950-969.

29. Silvestre, N. and Camotim D., *Shear deformable generalized beam theory for the analysis of thin-walled composite members.* Journal of Engineering Mechanics, 2012. **139**(8): p. 1010-1024.

30. Prokić, A., Lukić D., and Miličić I., *Free Vibration Analysis of Cross-Ply Laminated Thin-Walled Beams with Open Cross Sections: Exact Solution.* Journal of Structural Engineering, 2013. **623**.

31. Petrolo, M., Nagaraj M., Kaleel I., and Carrera E., *A global-local approach for the elastoplastic analysis of compact and thin-walled structures via refined models.* Computers & Structures, 2018. **206**: p. 54-65.

32. Carrera, E., Kaleel I., and Petrolo M., *Elastoplastic analysis of compact and thin-walled structures using classical and refined beam finite element models.* Mechanics of Advanced Materials and Structures, 2017: p. 1-13.

33. Carrera, E., de Miguel A., and Pagani A., *Extension of MITC to higher-order beam models and shear locking analysis for compact, thin-walled, and composite structures.* International Journal for Numerical Methods in Engineering, 2017. **112**(13): p. 1889-1908.

34. Filippi, M., Carrera E., and Regalli A.M., *Layerwise analyses of compact and thin-walled beams made of viscoelastic materials.* Journal of Vibration and Acoustics, 2016. **138**(6): p. 064501.

35. Carrera, E., Filippi M., Mahato P.K., and Pagani A., *Advanced models for free vibration analysis of laminated beams with compact and thin-walled open/closed sections.* Journal of Composite Materials, 2015. **49**(17): p. 2085-2101.

36. Sheikh, A.H., Asadi A., and Thomsen O.T., *Vibration of thin-walled laminated composite beams having open and closed sections.* Composite Structures, 2015. **134**: p. 209-215.

37. Li, X., Li Y., and Qin Y., *Free vibration characteristics of a spinning composite thin-walled beam under hygrothermal environment.* International Journal of Mechanical Sciences, 2016. **119**: p. 253-265.

38. Nguyen, T.-T., Thang P.T., and Lee J., *Lateral buckling analysis of thin-walled functionally graded open-section beams.* Composite Structures, 2017. **160**: p. 952-963.

39. Nguyen, T.-T., Kim N.-I., and Lee J., *Free vibration of thin-walled functionally graded open-section beams.* Composites Part B: Engineering, 2016. **95**: p. 105-116.

40. Lanc, D., Turkalj G., Vo T.P., and Brnić J., *Nonlinear buckling behaviours of thin-walled functionally graded open section beams.* Composite Structures, 2016. **152**: p. 829-839.

41. Kim, N.-I. and Lee J., *Investigation of coupled instability for shear flexible FG sandwich I-beams subjected to variable axial force.* Acta Mechanica, 2018. **229**(1): p. 47-70.

42. Kim, N.-I. and Lee J., *Coupled vibration characteristics of shear flexible thin-walled functionally graded sandwich I-beams.* Composites Part B: Engineering, 2017. **110**: p. 229-247.

43. Nguyen, T.-K., Nguyen N.-D., Vo T.P., and Thai H.-T., *Trigonometric-series*

solution for analysis of laminated composite beams. Composite Structures, 2017. **160**: p. 142-151.

44. Nguyen, N.-D., Nguyen T.-K., Nguyen T.-N., and Thai H.-T., *New Ritz-solution shape functions for analysis of thermo-mechanical buckling and vibration of laminated composite beams.* Composite Structures, 2017. **184**: p. 452-460.

45. Mantari, J. and Canales F., *Free vibration and buckling of laminated beams via hybrid Ritz solution for various penalized boundary conditions.* Composite Structures, 2016. **152**: p. 306-315.

46. Aydogdu, M., *Free vibration analysis of angle-ply laminated beams with general boundary conditions.* Journal of reinforced plastics and composites, 2006. **25**(15): p. 1571-1583.

47. Aydogdu, M., *Buckling analysis of cross-ply laminated beams with general boundary conditions by Ritz method.* Composites Science and Technology, 2006. **66**(10): p. 1248-1255.

48. Lee, J., *Center of gravity and shear center of thin-walled open-section composite beams.* Composite structures, 2001. **52**(2): p. 255-260.

49. Reddy, J.N., *Mechanics of laminated composite plates: theory and analysis.* 1997: CRC press.

50. Nguyen, T.-K., Sab K., and Bonnet G., *First-order shear deformation plate models for functionally graded materials.* Composite Structures, 2008. **83**(1): p. 25-36.

51. Hutchinson, J., *Shear coefficients for Timoshenko beam theory.* Journal of Applied Mechanics, 2001. **68**(1): p. 87-92.

52. Gruttmann, F. and Wagner W., *Shear correction factors in Timoshenko's beam theory for arbitrary shaped cross-sections.* Computational Mechanics, 2001. **27**(3):

p. 199-207.

53. Barbero, E.J., Lopez-Anido R., and Davalos J.F., *On the mechanics of thin-walled laminated composite beams.* Journal of Composite Materials, 1993. **27**(8): p. 806-829.

Figure Captions

Figure 1. Thin-walled coordinate systems

Figure 2. Geometry of thin-walled I-beams

Figure 3. Variation of the fundamental frequencies (Hz) of thin-walled C-C I-beams with respect to fiber angle.

Figure 4. Variation of the critical buckling loads (N) of thin-walled C-C I-beams with respect to fiber angle.

Figure 5. Shear effect on the fundamental frequency for various BCs

Figure 6. Shear effect on the critical buckling loads for various BCs

Figure 7. Shear effect on first three natural frequencies of thin-walled C-C I-beams

Figure 8. Variation of E_{33}/E_{77} ratio with respect to η

Figure 9. Mode shape 1 of thin-walled C-C I-beams

Figure 10. Mode shape 2 of thin-walled C-C I-beams

Figure 11. Mode shape 3 of thin-walled C-C I-beams

Figure 12. Non-dimensional fundamental frequency for various BCs

Figure 13. Non-dimensional critical buckling load for various BCs

Figure 14. Non-dimensional fundamental frequency of thin-walled FG sandwich I-beams.

Figure 15. Non-dimensional fundamental frequency with respect to α_1, α_2 ($\alpha_1 = \alpha_2, \beta = 0.3$ and $p = 10$)

Figure 16. Non-dimensional critical buckling load with respect to α_1, α_2 ($\beta = 0.3$ and $p = 10$)

Table Captions

Table 1. Shape functions and essential BCs of thin-walled I-beams.

Table 2. Material properties of thin-walled I-beams.

Table 3. Convergence studies for thin-walled composite and FG sandwich I-beams.

Table 4. The fundamental frequency (Hz) of thin-walled S-S and C-F I-beams

Table 5. Critical buckling load (N) of thin-walled S-S and C-F I-beams

Table 6. Non-dimensional natural frequency of thin-walled S-S I-beams

Table 7. Non-dimensional natural frequency of thin-walled C-F I-beams

Table 8. Non-dimensional natural frequency of thin-walled C-C I-beams

Table 9. Non-dimensional critical buckling load of thin-walled composite I-beams

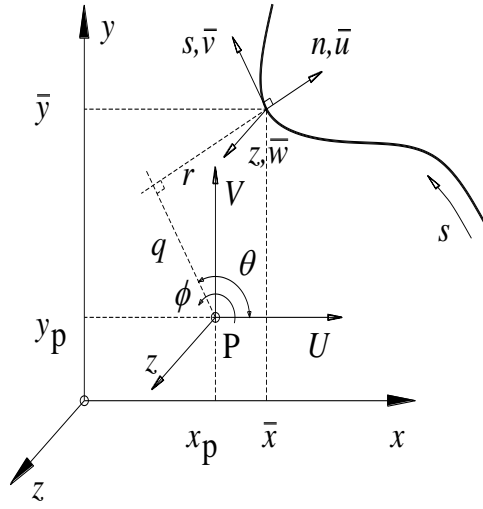Table 10. The critical buckling load (N) of FG sandwich I-beams
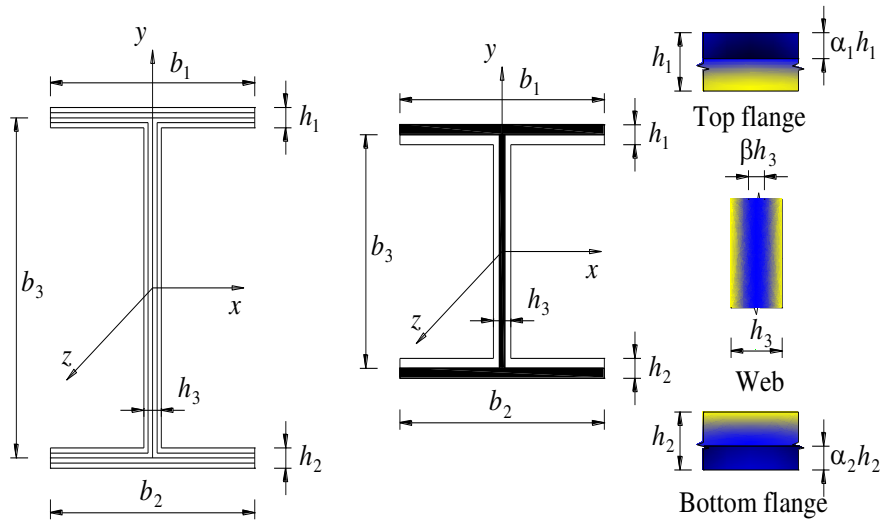
Figure 1. Thin-walled coordinate systems

a. Composite I-beams   b. FG sandwich I-beams
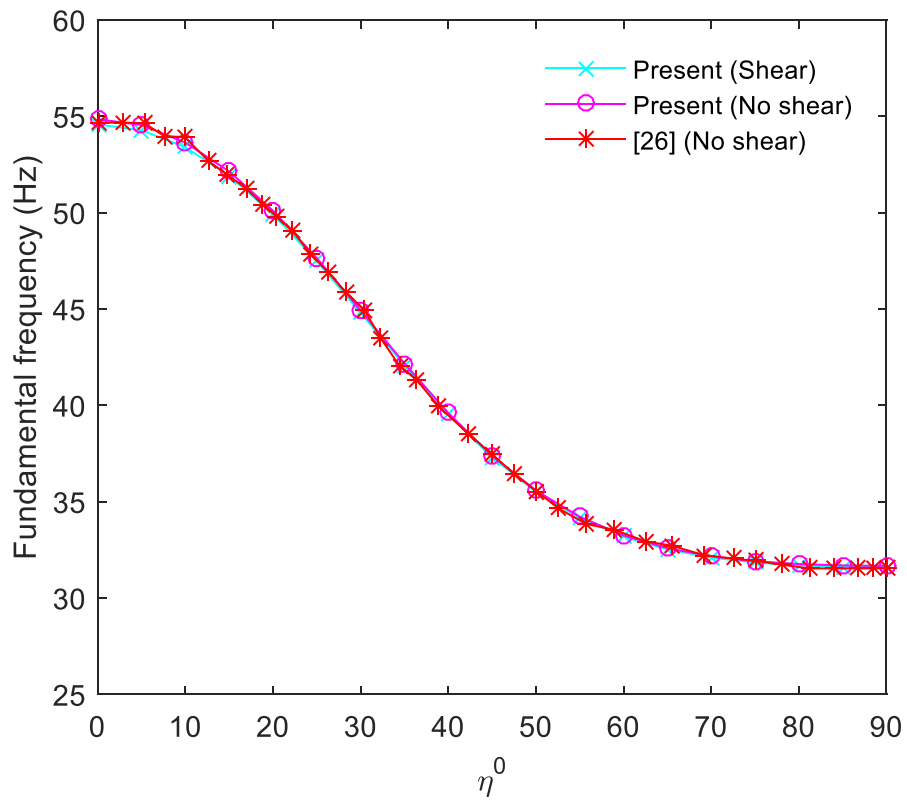
Figure 2. Geometry of thin-walled I-beams

Figure 3. Variation of the fundamental frequencies (Hz) of thin-walled C-C I-beams with respect to fiber angle.

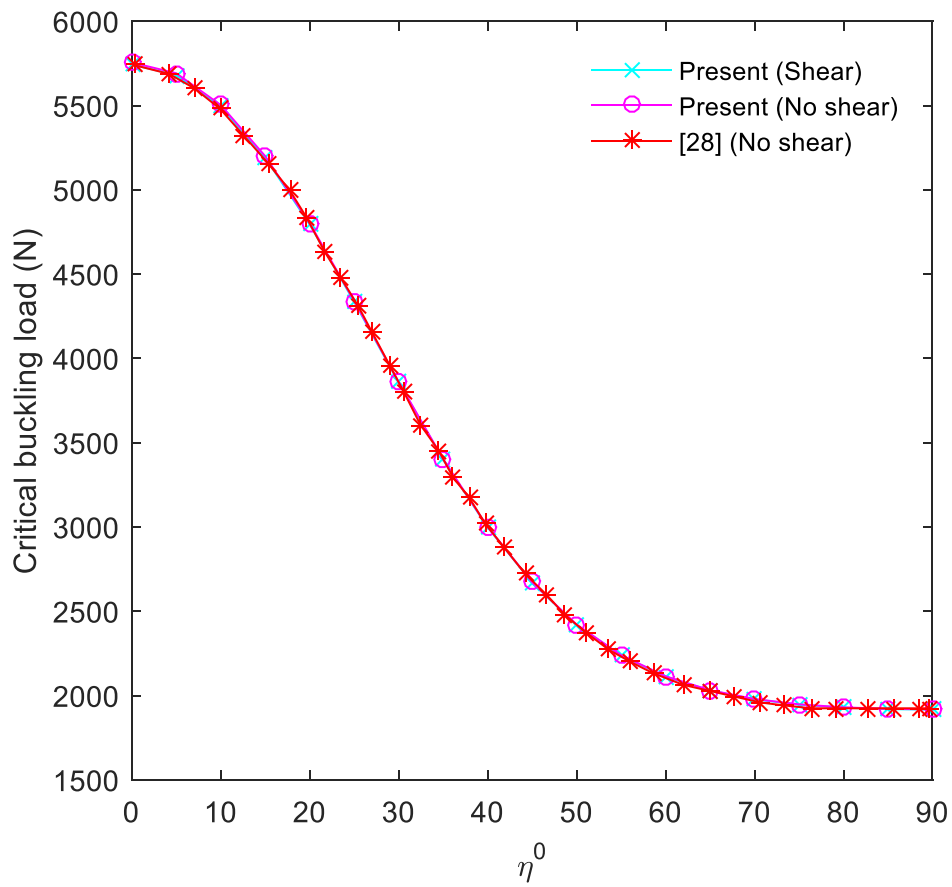Figure 4. Variation of the critical buckling loads (N) of thin-walled C-C I-beams with respect to fiber angle.

Figure 5. Shear effect on the fundamental frequency for various BCs
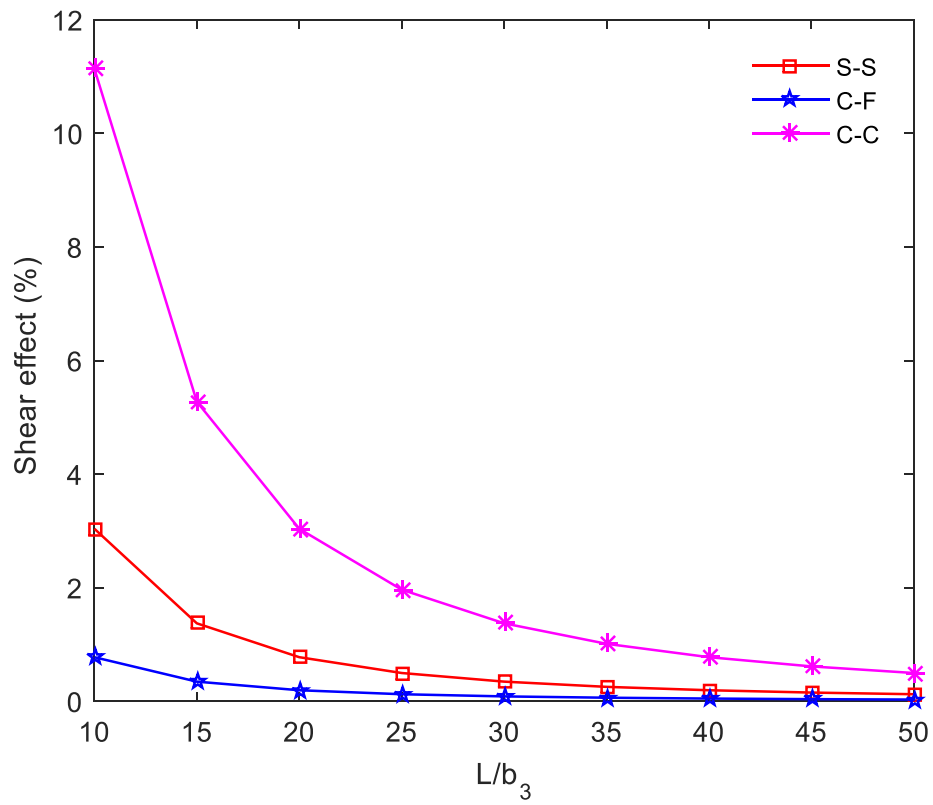
Figure 6. Shear effect on the critical buckling loads for various BCs

Figure 7. Shear effect on first three natural frequencies of thin-walled C-C I-beams
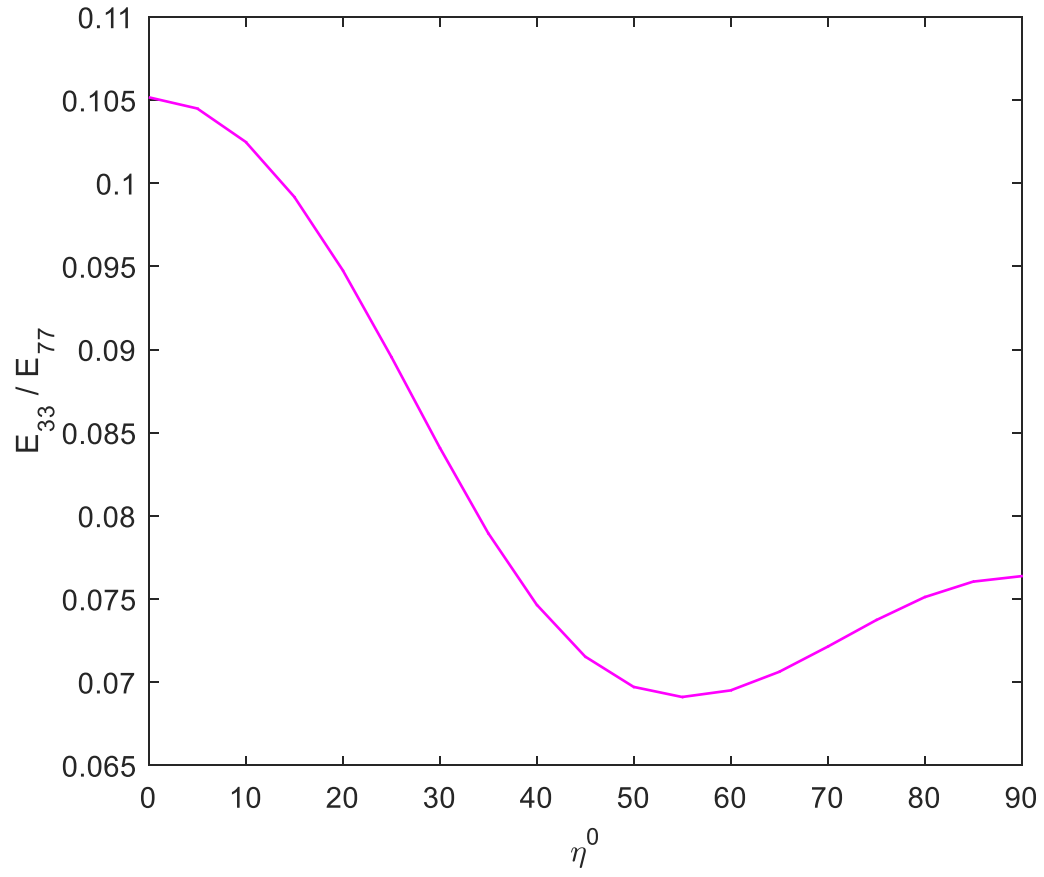
Figure 8. Variation of E_{33}/E_{77} ratio with respect to η
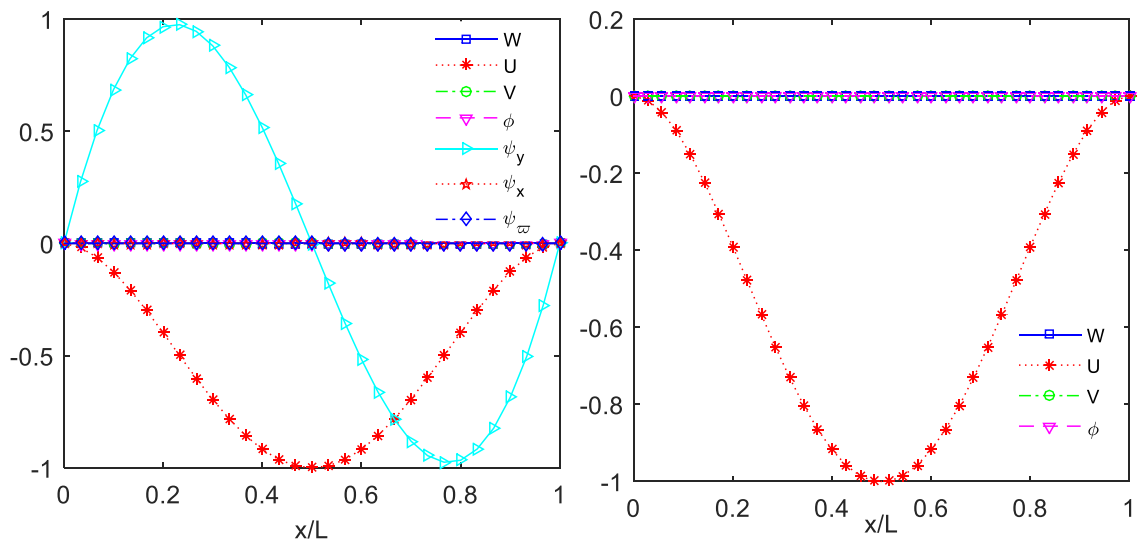
a. $\bar{\omega}_1 = 6.049$ (Shear)

b. $\bar{\omega}_1 = 6.239$ (No shear)

Figure 9. Mode shape 1 of thin-walled C-C I-beams
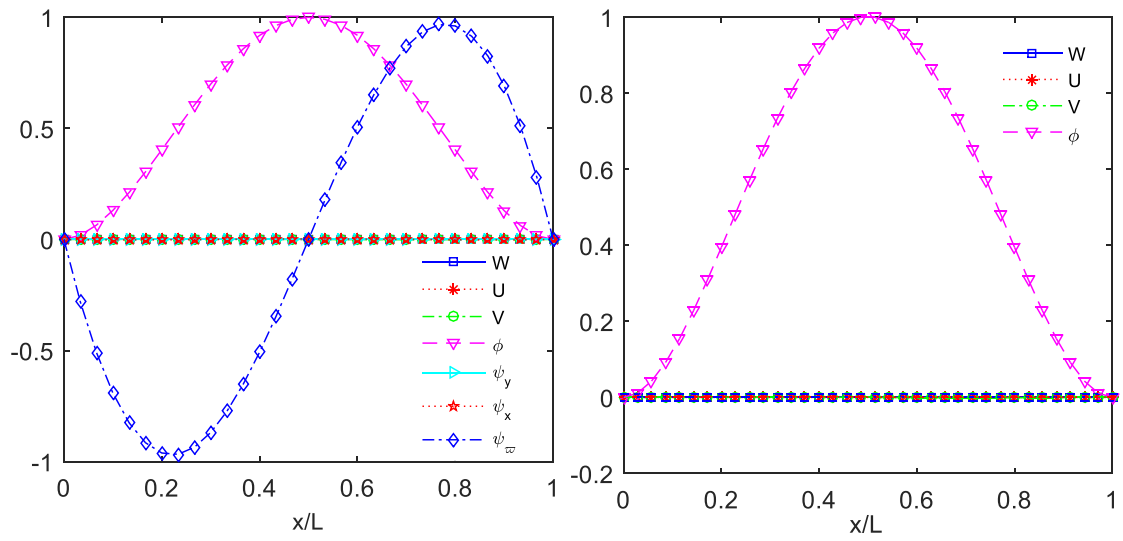
a. $\bar{\omega}_2 = 6.383$ (Shear)   b. $\bar{\omega}_2 = 6.596$ (No shear)

Figure 10. Mode shape 2 of thin-walled C-C I-beams
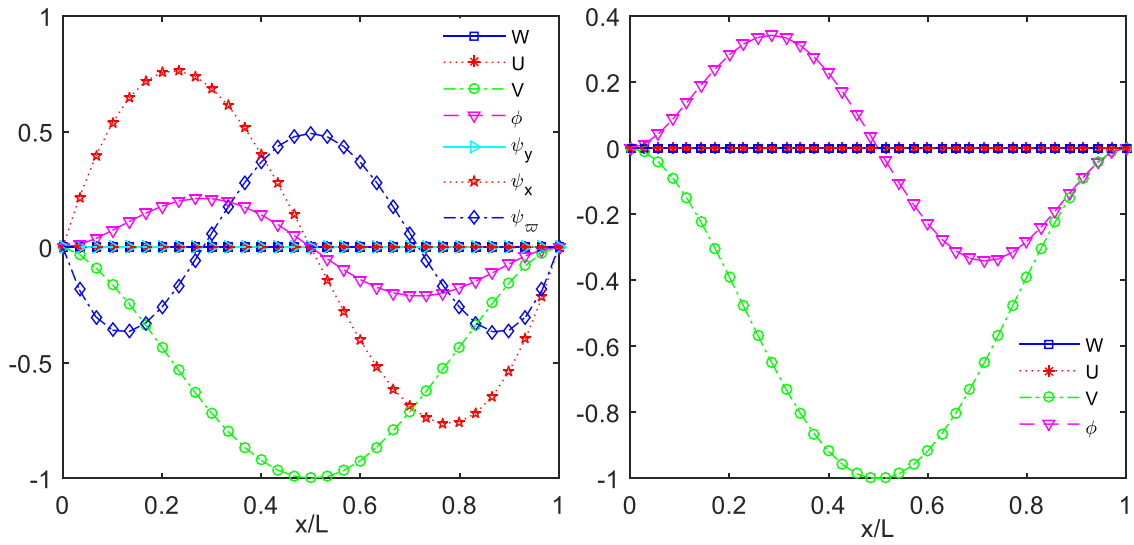
a. $\bar{\omega}_3 = 10.607$ (Shear) b. $\bar{\omega}_3 = 12.555$ (No shear)

Figure 11. Mode shape 3 of thin-walled C-C I-beams
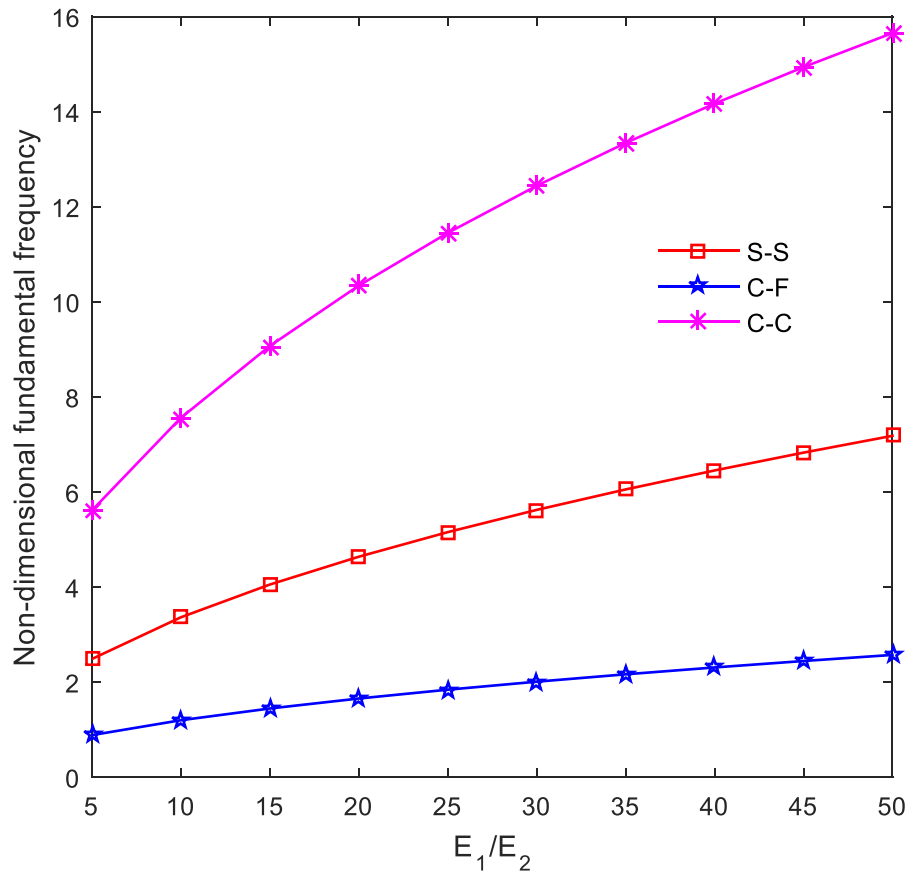
Figure 12. Non-dimensional fundamental frequency for various BCs
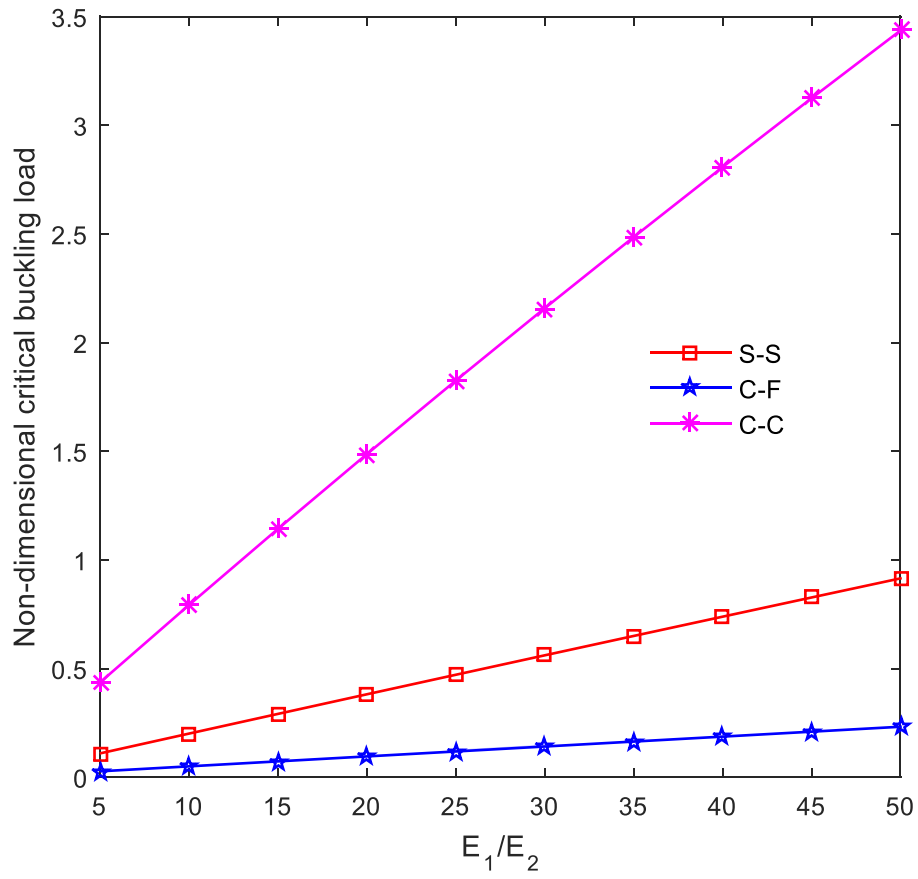
Figure 13. Non-dimensional critical buckling load for various BCs
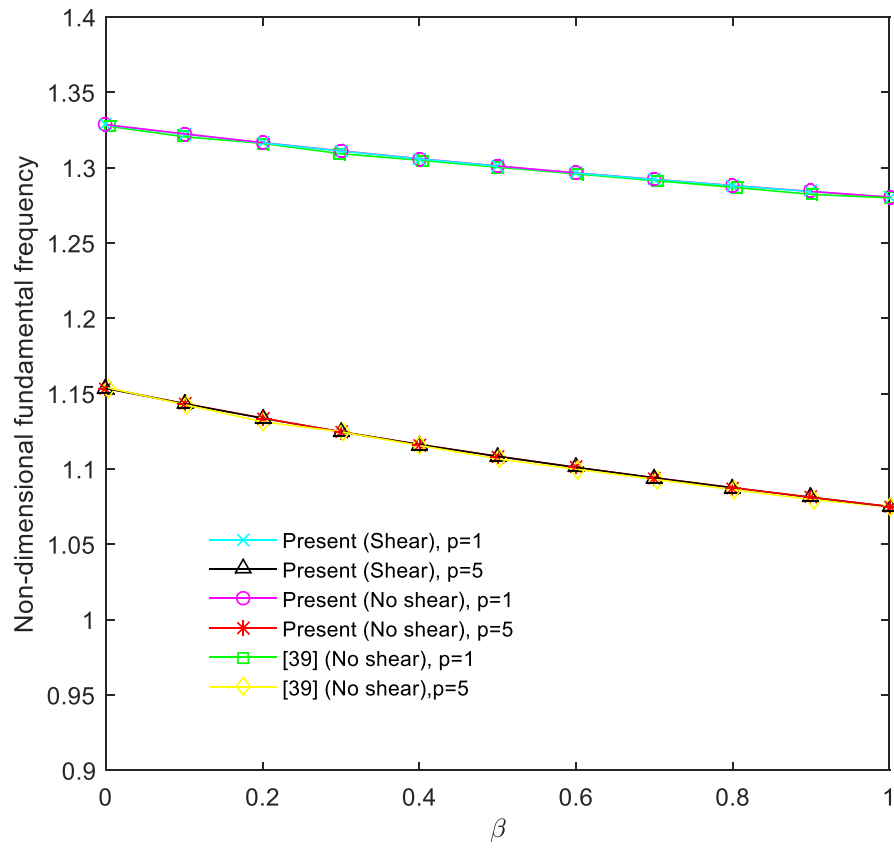
Figure 14. Non-dimensional fundamental frequency of thin-walled FG sandwich I-beams.
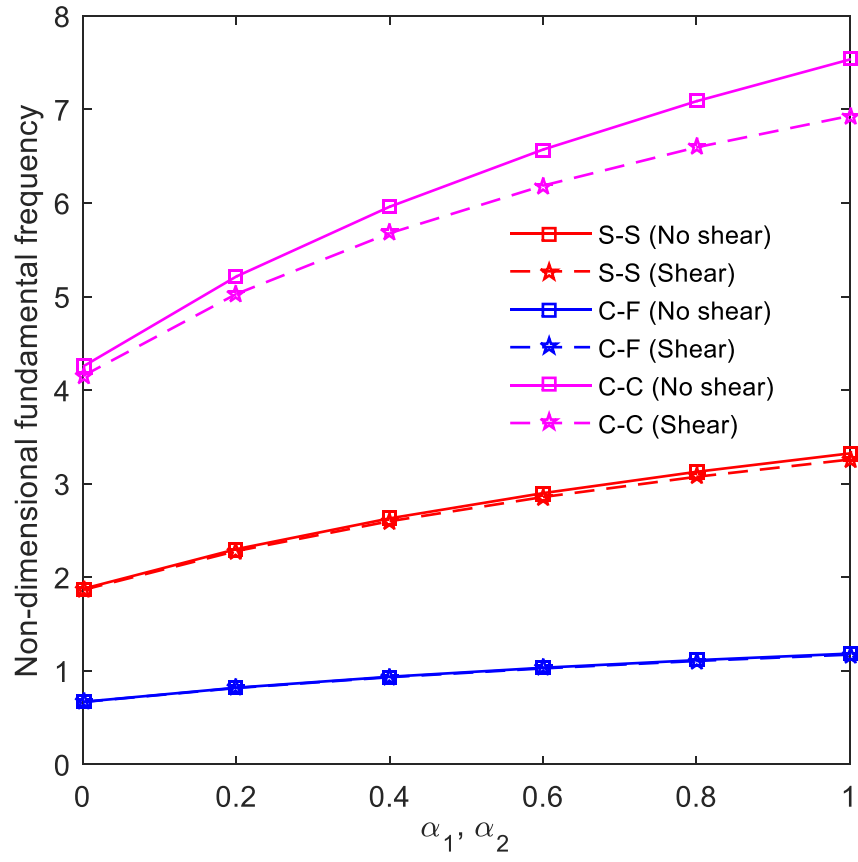
Figure 15. Non-dimensional fundamental frequency with respect to α_1, α_2 ($\alpha_1 = \alpha_2$, $\beta = 0.3$ and $p = 10$)
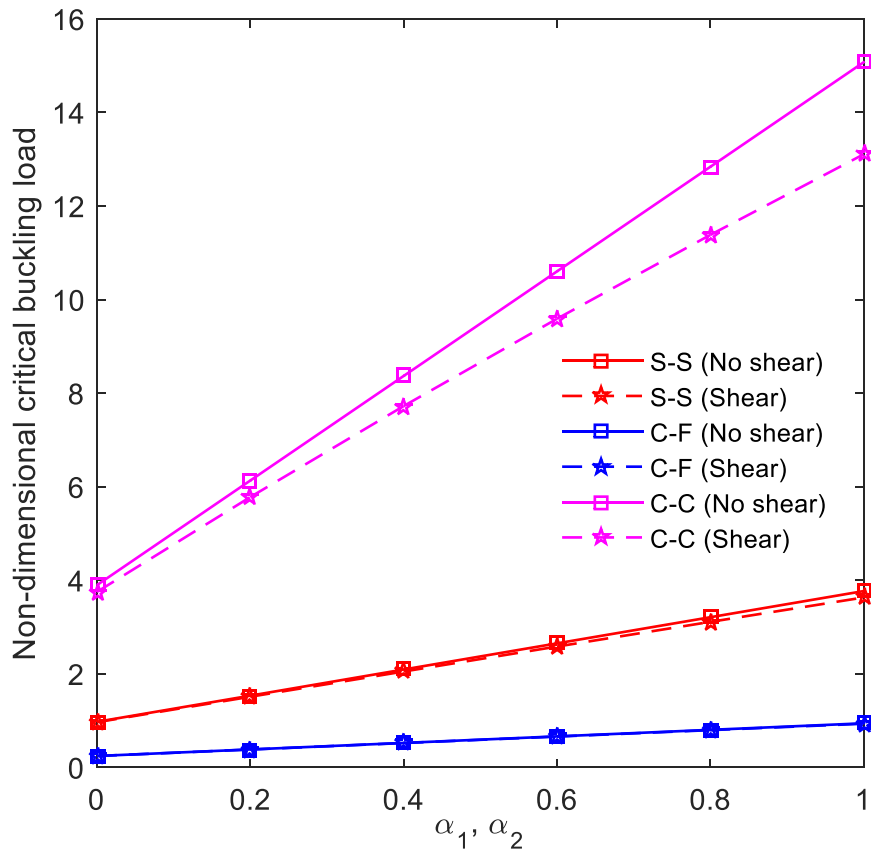
Figure 16. Non-dimensional critical buckling load with respect to α_1, α_2 ($\beta = 0.3$ and $p = 10$)
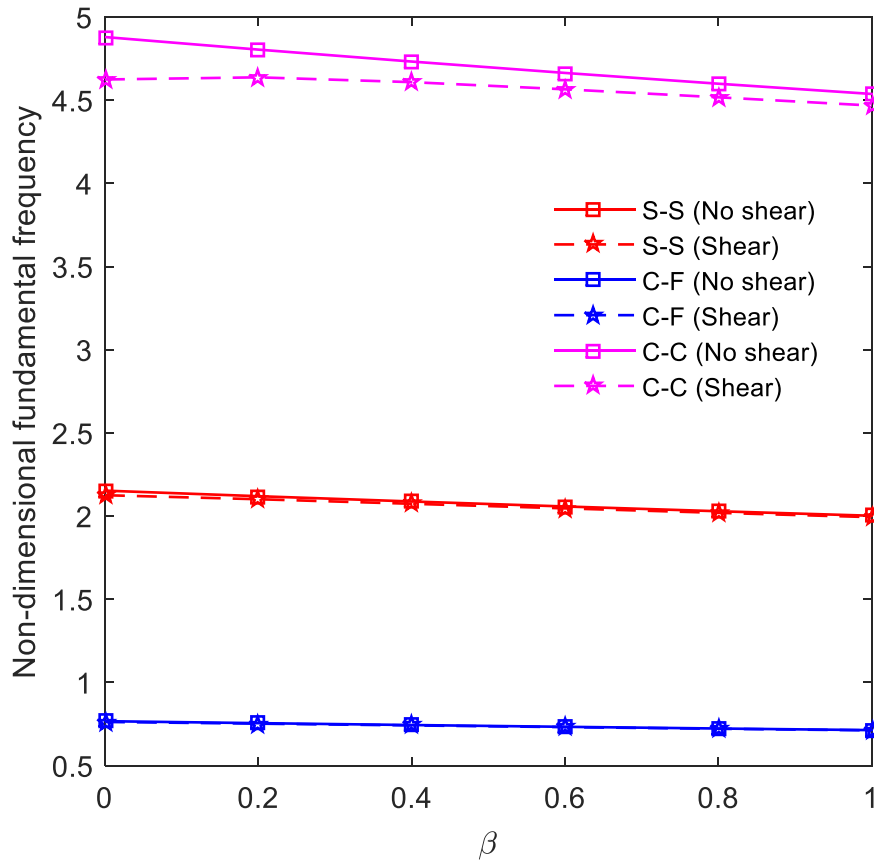
Figure 17. Non-dimensional fundamental frequency with respect to β ($\alpha_1 = \alpha_2 = 0.1$, and $p = 10$)
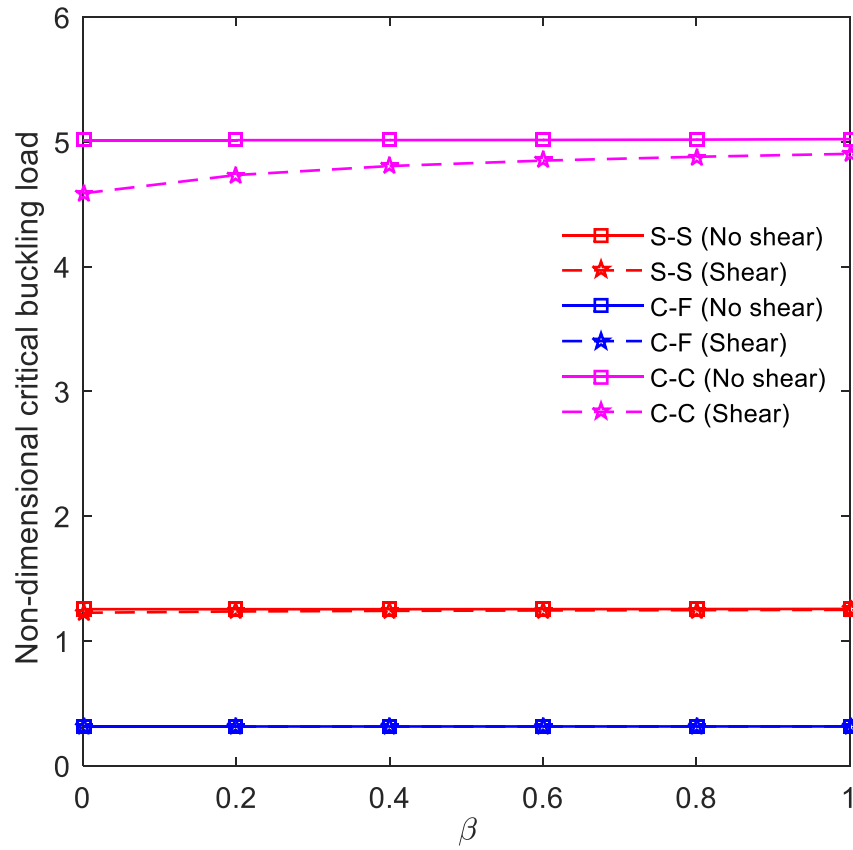
Figure 18. Non-dimensional critical buckling load with respect to β ($\alpha_1 = \alpha_2 = 0.1$, and $p = 10$)
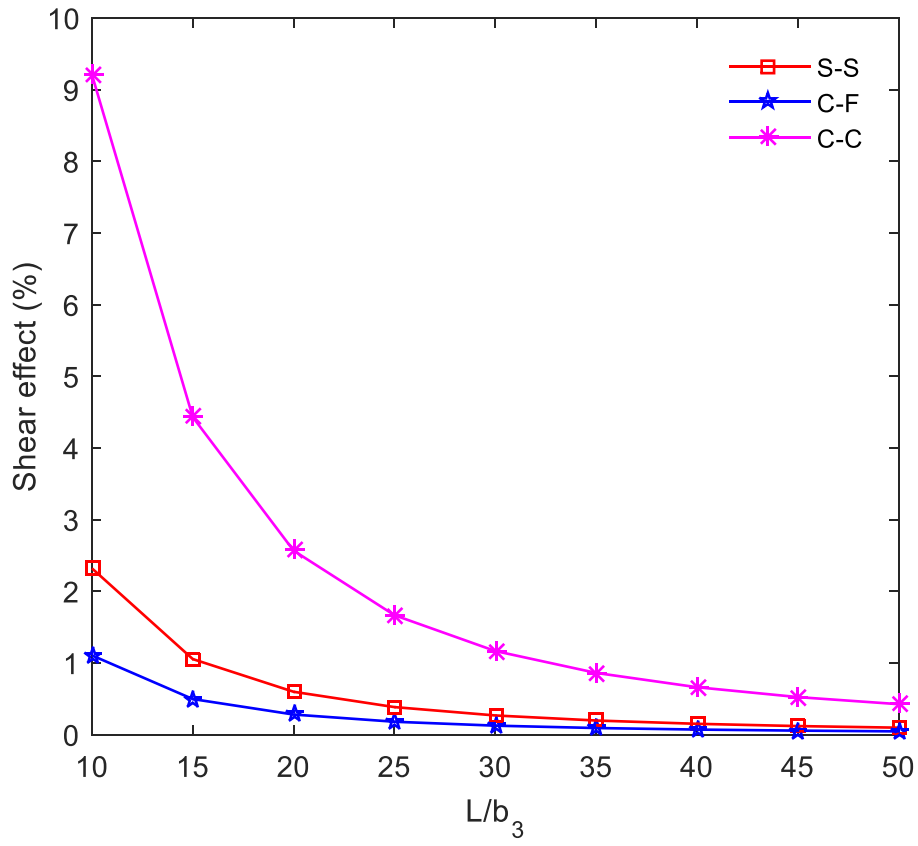
Figure 19. Shear effect on fundamental frequency for various BCs
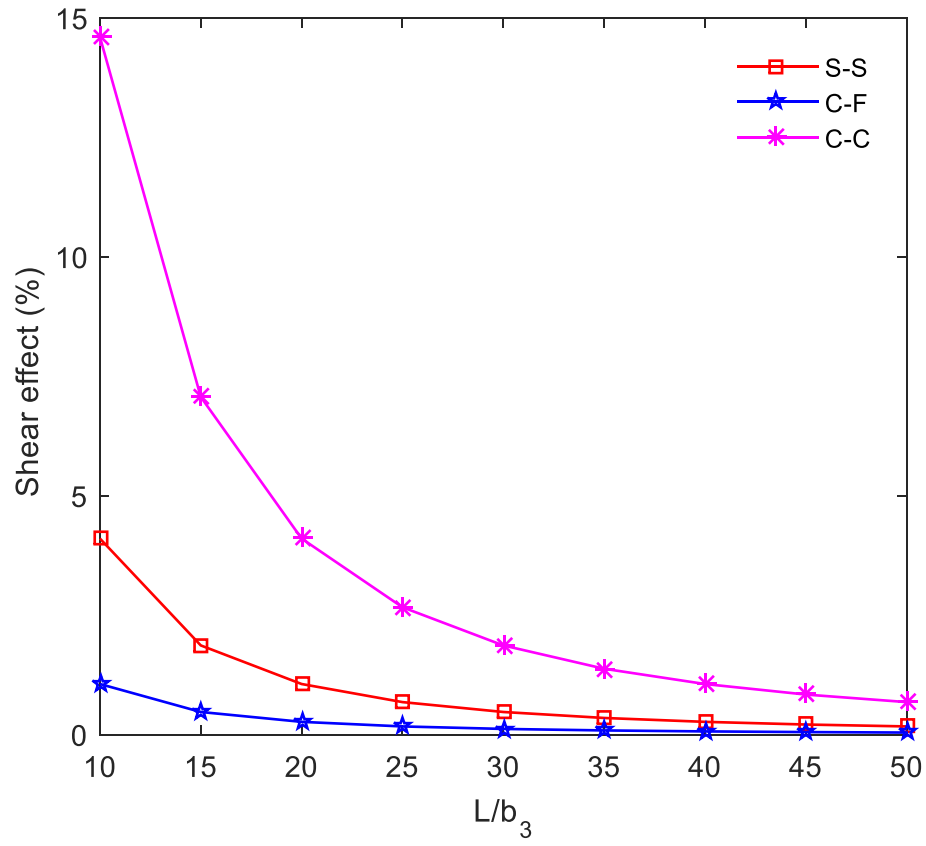
Figure 20. Shear effect on critical buckling load for various BCs
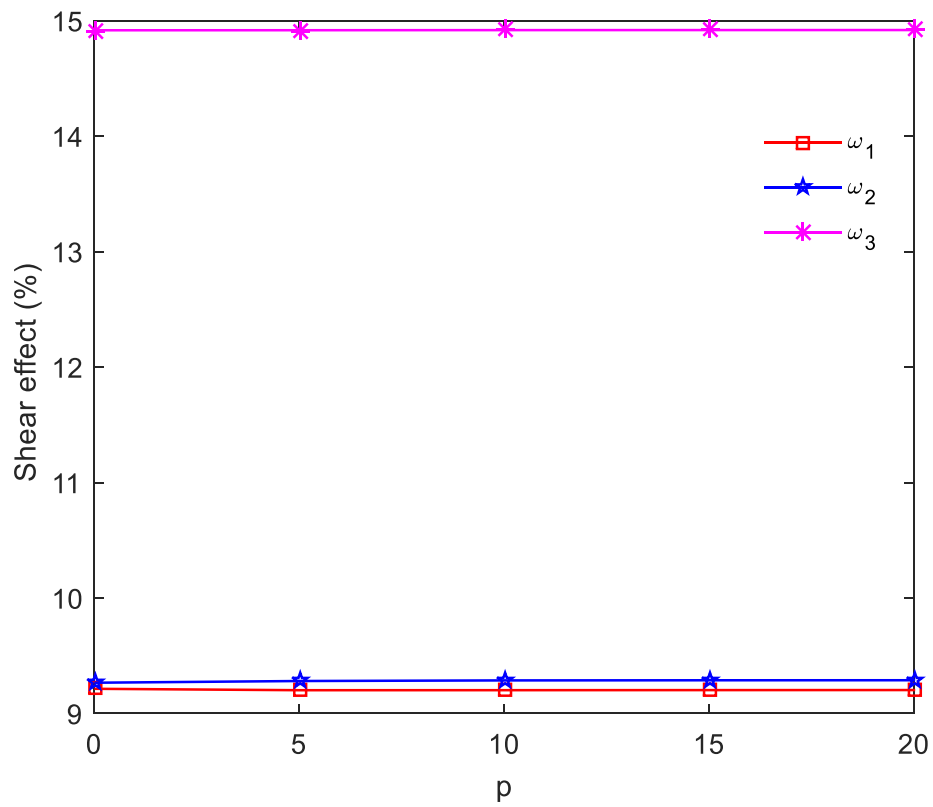
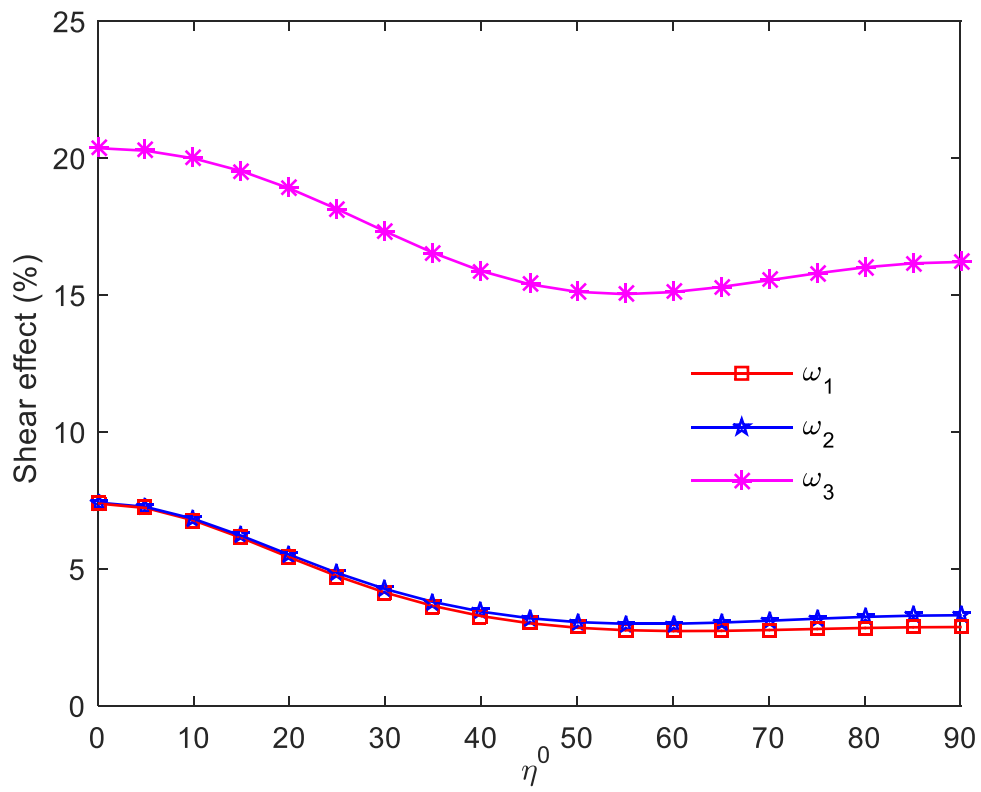Figure 21. Shear effect on first three frequency of C-C I-beams with respect to material parameter

Table 1. Shape functions and essential BCs of thin-walled I-beams.

BC	$\dfrac{\varphi_j(x)}{e^{\frac{-jx}{L}}}$	$x=0$	$x=L$
S-S	$\dfrac{x}{L}\left(1-\dfrac{x}{L}\right)$	$U=V=\phi=0$	$U=V=\phi=0$
C-F	$\left(\dfrac{x}{L}\right)^2$	$U=V=\phi=0$ $U'=V'=\phi'=0$ $W=\psi_y=\psi_x=\psi_\varpi=0$	
C-C	$\left(\dfrac{x}{L}\right)^2\left(1-\dfrac{x}{L}\right)^2$	$U=V=\phi=0$ $U'=V'=\phi'=0$ $W=\psi_y=\psi_x=\psi_\varpi=0$	$U=V=\phi=0$ $U'=V'=\phi'=0$ $W=\psi_y=\psi_x=\psi_\varpi=0$

Table 2. Material properties of thin-walled I-beams.

Material properties	MAT I	MAT II	MAT III	MAT IV
E_1, E_c (GPa)	53.78	25	380	320.7
$E_2 = E_3$, E_m (GPa)	17.93	1	70	101.69
$G_{12} = G_{13}$ (GPa)	8.96	0.6	-	-
G_{23} (GPa)	3.45	0.6	-	-
v, $v_{12} = v_{13}$	0.25	0.25	0.30	0.3
ρ (kg/m^3)	1968.90	-	-	-
ρ_c (kg/m^3)	-	-	3960	-
ρ_m (kg/m^3)	-	-	2702	-

Table 3. Convergence studies for thin-walled composite and FG sandwich I-beams.

BC		*m*					
		2	4	6	8	10	12
1. Thin-walled composite I-beams							
a. Fundamental frequency (Hz)							
S-S	Shear	16.763	16.544	16.482	16.481	16.481	16.481
	No shear	16.773	16.553	16.491	16.490	16.490	16.490
C-F	Shear	5.958	5.878	5.873	5.873	5.873	5.873
	No shear	5.959	5.880	5.875	5.875	5.875	5.875
C-C	Shear	37.433	37.307	37.304	37.303	37.302	37.301
	No shear	37.502	37.382	37.382	37.382	37.382	37.382
b. Critical buckling load (kN)							
S-S	Shear	2.752	2.690	2.671	2.671	2.671	2.671
	No shear	2.755	2.692	2.673	2.673	2.673	2.673
C-F	Shear	0.706	0.668	0.668	0.668	0.668	0.668
	No shear	0.706	0.668	0.668	0.668	0.668	0.668
C-C	Shear	10.797	10.678	10.657	10.657	10.657	10.657
	No shear	10.832	10.712	10.691	10.691	10.691	10.691
2. Thin-walled functionally graded sandwich I-beams							
a. Fundamental frequency (Hz)							
S-S	Shear	92.715	91.522	91.184	91.180	91.180	91.180
	No shear	93.701	92.474	92.127	92.122	92.122	92.122
C-F	Shear	33.137	32.690	32.663	32.660	32.660	32.660
	No shear	33.291	32.846	32.820	32.818	32.818	32.818
C-C	Shear	201.801	200.434	200.127	199.973	199.885	199.830
	No shear	209.499	208.830	208.828	208.828	208.828	208.828
b. Critical buckling load (MN)							
S-S	Shear	1.036	1.013	1.006	1.006	1.006	1.006
	No shear	1.055	1.031	1.024	1.024	1.024	1.024
C-F	Shear	0.269	0.255	0.255	0.255	0.255	0.255
	No shear	0.271	0.256	0.256	0.256	0.256	0.256
C-C	Shear	3.867	3.827	3.820	3.820	3.820	3.820
	No shear	4.150	4.104	4.096	4.096	4.096	4.096

Table 4. The fundamental frequency (Hz) of thin-walled S-S and C-F I-beams

BC	Reference	Lay-up						
		$[0]_{16}$	$\begin{bmatrix}15/\\-15\end{bmatrix}_{4s}$	$\begin{bmatrix}30/\\-30\end{bmatrix}_{4s}$	$\begin{bmatrix}45/\\-45\end{bmatrix}_{4s}$	$\begin{bmatrix}60/\\-60\end{bmatrix}_{4s}$	$\begin{bmatrix}75/\\-75\end{bmatrix}_{4s}$	$\begin{bmatrix}90/\\-90\end{bmatrix}_{4s}$
S-S	Present (Shear)	24.169	22.977	19.806	16.481	14.660	14.071	13.964
	Present (No shear)	24.198	23.001	19.820	16.490	14.668	14.079	13.972
	Vo and Lee [24] (Shear)	24.150	22.955	19.776	16.446	14.627	14.042	13.937
	Sheikh et al. [36] (Shear)	24.160	22.970	19.800	16.480	14.660	14.070	13.960
	Kim et al. [26] (No shear)	24.194	22.997	19.816	16.487	14.666	14.077	13.970
C-F	Present (Shear)	26.479	25.174	21.699	18.057	16.063	15.417	15.299
	Present (No shear)	26.514	25.202	21.717	18.069	16.072	15.427	15.309
	Kim and Lee [9] (Shear)	26.460	25.160	21.700	18.060	16.060	15.420	15.300
	Kim and Lee [9] (No shear)	26.510	25.200	21.710	18.070	16.070	15.420	15.310

Table 5. Critical buckling load (N) of thin-walled S-S and C-F I-beams

BC	Reference	Lay-up						
		$[0]_{16}$	$\begin{bmatrix}15/\\-15\end{bmatrix}_{4s}$	$\begin{bmatrix}30/\\-30\end{bmatrix}_{4s}$	$\begin{bmatrix}45/\\-45\end{bmatrix}_{4s}$	$\begin{bmatrix}60/\\-60\end{bmatrix}_{4s}$	$\begin{bmatrix}75/\\-75\end{bmatrix}_{4s}$	$\begin{bmatrix}0/\\90\end{bmatrix}_{4s}$
S-S	Present (Shear)	1438.1	1299.4	965.0	668.1	528.6	487.0	959.0
	Present (No shear)	1438.8	1300.0	965.2	668.2	528.7	487.1	959.3
	Kim et al. [27] (No shear)	1438.8	1300.0	965.2	668.2	528.7	487.1	964.4
C-F	Present (Shear)	5743.3	5191.0	3856.8	2670.6	2113.2	1946.7	3831.4
	Present (No shear)	5755.2	5199.7	3861.0	2672.7	2114.7	1948.3	3837.3
	Vo and Lee [24] (Shear)	5741.5	5189.0	3854.5	2668.4	2111.3	1945.1	3829.8
	Kim et al. [27] (No shear)	5755.2	5199.8	3861.0	2672.7	2114.7	1948.3	3857.8

Table 6. Non-dimensional natural frequency of thin-walled S-S I-beams

Reference	Frequency	Lay-up						
		$[0]$	$\begin{bmatrix}15/\\-15\end{bmatrix}$	$\begin{bmatrix}30/\\-30\end{bmatrix}$	$\begin{bmatrix}45/\\-45\end{bmatrix}$	$\begin{bmatrix}60/\\-60\end{bmatrix}$	$\begin{bmatrix}75/\\-75\end{bmatrix}$	$\begin{bmatrix}90/\\-90\end{bmatrix}$
Present (Shear)	ω_1	7.107	6.327	3.755	2.151	1.627	1.493	1.468
	ω_2	8.189	7.528	5.137	3.610	2.967	2.713	2.645
	ω_3	19.140	17.594	12.904	8.583	6.495	5.958	5.860
	ω_4	27.542	24.998	14.957	10.445	8.577	7.849	7.685
	ω_5	30.741	28.408	17.791	11.078	9.976	9.841	9.817
Present (No shear)	ω_1	7.186	6.353	3.761	2.153	1.628	1.494	1.469
	ω_2	8.303	7.561	5.145	3.614	2.970	2.715	2.648
	ω_3	20.856	18.903	13.404	8.611	6.513	5.974	5.876
	ω_4	28.743	25.412	15.043	10.654	8.606	7.876	7.713
	ω_5	32.408	28.935	17.917	11.191	10.213	10.069	10.045

Table 7. Non-dimensional natural frequency of thin-walled C-F I-beams

Reference	Frequency	Lay-up						
		$[0]$	$\begin{bmatrix}15/\\-15\end{bmatrix}$	$\begin{bmatrix}30/\\-30\end{bmatrix}$	$\begin{bmatrix}45/\\-45\end{bmatrix}$	$\begin{bmatrix}60/\\-60\end{bmatrix}$	$\begin{bmatrix}75/\\-75\end{bmatrix}$	$\begin{bmatrix}90/\\-90\end{bmatrix}$
Present (Shear)	ω_1	2.547	2.259	1.339	0.767	0.580	0.532	0.523
	ω_2	3.174	3.057	2.423	1.877	1.572	1.438	1.400
	ω_3	7.123	6.538	4.746	3.821	3.597	3.327	3.272
	ω_4	15.492	13.995	8.357	4.793	3.627	3.548	3.540
	ω_5	17.559	16.307	10.755	7.177	5.780	5.285	5.162
Present (No shear)	ω_1	2.560	2.263	1.340	0.767	0.580	0.532	0.523
	ω_2	3.197	3.064	2.426	1.879	1.574	1.439	1.401
	ω_3	7.430	6.772	4.835	3.896	3.635	3.335	3.280
	ω_4	16.043	14.183	8.396	4.806	3.637	3.587	3.578
	ω_5	18.333	16.549	10.811	7.199	5.796	5.300	5.177

Table 8. Non-dimensional natural frequency of thin-walled C-C I-beams

Reference	Frequency	$[0]$	$\begin{bmatrix}15/\\-15\end{bmatrix}$	$\begin{bmatrix}30/\\-30\end{bmatrix}$	$\begin{bmatrix}45/\\-45\end{bmatrix}$	$\begin{bmatrix}60/\\-60\end{bmatrix}$	$\begin{bmatrix}75/\\-75\end{bmatrix}$	$\begin{bmatrix}90/\\-90\end{bmatrix}$
Present (Shear)	ω_1	15.480	14.129	8.474	4.865	3.682	3.378	3.322
	ω_2	17.239	16.086	10.104	6.206	4.839	4.423	4.332
	ω_3	34.221	32.379	23.221	13.368	10.121	9.285	9.131
	ω_4	40.918	38.293	25.221	15.901	12.265	11.221	11.004
	ω_5	44.983	43.101	27.483	22.047	19.739	18.106	17.804
Present (No shear)	ω_1	16.289	14.401	8.525	4.880	3.691	3.386	3.330
	ω_2	18.362	16.429	10.172	6.228	4.854	4.438	4.346
	ω_3	44.902	39.698	23.499	13.452	10.175	9.334	9.180
	ω_4	47.279	42.154	26.604	16.021	12.342	11.294	11.079
	ω_5	50.406	45.561	31.022	24.622	19.946	18.298	17.996
Vo and Lee [24] (Shear)	ω_1	15.460	14.122	8.471	4.862	3.678	3.374	3.319
	ω_2	17.211	16.064	10.092	6.202	4.836	4.421	4.330
	ω_3	33.996	32.174	23.209	13.392	10.147	9.308	9.152
	ω_4	40.271	38.063	25.126	15.919	12.286	11.239	11.022
	ω_5	44.134	42.818	27.457	21.991	19.855	18.211	17.905
Vo and Lee [24] (No shear)	ω_1	16.289	14.401	8.525	4.880	3.691	3.386	3.330
	ω_2	18.362	16.429	10.172	6.228	4.854	4.438	4.346
	ω_3	44.903	39.698	23.499	13.452	10.175	9.334	9.180
	ω_4	47.279	42.154	26.604	16.021	12.342	11.294	11.079
	ω_5	50.406	45.561	31.022	24.622	19.946	18.298	17.996

Table 9. Non-dimensional critical buckling load of thin-walled composite I-beams

BC	Reference	Lay-up						
		$[0]$	$\begin{bmatrix} 15/ \\ -15 \end{bmatrix}$	$\begin{bmatrix} 30/ \\ -30 \end{bmatrix}$	$\begin{bmatrix} 45/ \\ -45 \end{bmatrix}$	$\begin{bmatrix} 60/ \\ -60 \end{bmatrix}$	$\begin{bmatrix} 75/ \\ -75 \end{bmatrix}$	$\begin{bmatrix} 90/ \\ -90 \end{bmatrix}$
S-S	Present (Shear)	11.947	9.468	3.336	1.094	0.626	0.527	0.510
	Present (No shear)	12.208	9.542	3.344	1.096	0.627	0.527	0.510
C-F	Present (Shear)	3.035	2.381	0.835	0.274	0.157	0.132	0.128
	Present (No shear)	3.052	2.385	0.836	0.274	0.157	0.132	0.128
C-C	Present (Shear)	44.914	37.007	13.249	4.363	2.498	2.102	2.034
	Present (No shear)	48.830	38.167	13.374	4.383	2.507	2.110	2.041

Table 10. The critical buckling load (N) of FG sandwich I-beams

BC	p	Reference				
		Present		Kim and Lee [41]		Lanc et al. [40]
		Shear	No shear	Shear	No shear	No shear
S-S	0	421633	423079	422359	423083	423296
	0.25	404154	405602	405208	405933	406130
	0.5	392508	393960	393783	394515	394692
	1	377958	379420	379533	380286	380412
	2	363420	364899	365280	366056	366150
	5	348899	350404	351058	351825	351914
	10	342305	343826	344601	345333	345451
	20	338539	340070	340906	341605	341762
C-F	0	105679	105770	105725	105771	105773
	0.25	101310	101401	101435	101483	101484
	0.5	98399	98490	98577	98629	98626
	1	94763	94855	95013	95072	95057
	2	91132	91225	91448	91514	91494
	5	87507	87601	87891	87957	87936
	10	85861	85957	86277	86334	86321
	20	84922	85018	85353	85403	85400
C-C	0	1669413	1692317	1680840	1692352	1705050
	0.25	1599491	1622408	1612410	1623751	1635900
	0.5	1552860	1575838	1566830	1578078	1589830
	1	1494551	1517678	1509950	1521156	1532310
	2	1436213	1459595	1453060	1464229	1474860
	5	1377838	1401613	1396270	1407293	1417520
	10	1351288	1375299	1370490	1381317	1391480
	20	1336111	1360275	1355730	1366399	1376630